NAA-SR-8399

SNAP 10A-PSM-1 TEST RESULTS

AEC Research and Development Report

ATOMICS INTERNATIONAL

A DIVISION OF NORTH AMERICAN AVIATION, INC.

DISCLAIMER

LEGAL NOTICE

Price $2.00
Available from the Office of Technical Services
Department of Commerce
Washington 25, D. C.

NAA-SR-8399
REACTOR TECHNOLOGY
TID-4500 (29th Ed.)
SNAP REACTOR,
SNAP PROGRAM
M-3679 (34th Ed.)
87 PAGES

SNAP 10A-PSM-1 TEST RESULTS

By
R.M. OLIVA

ATOMICS INTERNATIONAL

A DIVISION OF NORTH AMERICAN AVIATION, INC.
P.O. BOX 309 CANOGA PARK, CALIFORNIA

CONTRACT: AT(11-1)-GEN-8
ISSUED: JUL 15 1964

DISTRIBUTION

This report has been distributed according to the category Reactor Technology, UC-80, as given in "Standard Distribution for Unclassified Scientific and Technical Reports," TID-4500 (29th Edition), April 1, 1964, with nonduplicating distribution from the category SNAP Reactors, SNAP Program, C-92b, given in "Standard Distribution for Classified Scientific and Technical Reports," M-3679 (34th Edition), March 15, 1964. A total of 725 copies was printed.

CONTENTS

TABLES

TABLES

FIGURES

FIGURES

FIGURES

I. INTRODUCTION

On November 14, 1961, an environmental test program commenced on the first SNAP 10A system structure, S10A-PSM-1. The object of this test was to subject the test vehicle to specified vibration, shock, and acceleration inputs and thereby determine various structural characteristics, such as major resonant frequencies, damping rates, magnification factors at various vehicle locations, stress levels at various preselected points, and deflections of structure and components under static (acceleration) loads. The results of these tests would be useful in verifying the integrity of the design tested and would yield information invaluable to the analysis and design of this and future SNAP 10A systems.

Initial testing was performed on the large vibration shaker with inputs applied through the test vehicle's longitudinal (Z-Z) axis.* These first tests consisted of running low-level surveys to obtain response and strain data from the many sensors located on the test vehicle. Because of the limited supply of data acquisition equipment and the many instrumentation locations required, it was necessary to conduct numerous tests in order to accumulate data at all sensor stations. Before the entire array of points could be surveyed and prior to application of any vibration inputs in the lateral or normal axes, internal shield damage occurred. The shield was removed and a dummy unit was installed for the remaining tests.

Following the longitudinal low level test program, the unit was mounted on the slip table and the vehicle surveyed with vibration input applied laterally at the base. A 50% test run was conducted after low-level surveys of both strain gages and accelerometers had been completed.

Once the tests with lateral inputs were concluded, the vehicle was rotated 90° on the slip plate so that vibration tests could be conducted through the third and final vehicle axis. Since the PSM-1 test unit was essentially symmetrical about either the lateral (Y-Y) or normal (X-X) axes, low-level surveys in this third attitude were minimized after it was established that

*At the time of this test, axis identification was as follows: longitudinal (Z-Z), lateral (Y-Y), and normal (X-X). This report retains this designation. Follow-on SNAP systems used a different axis identification.

similar vehicle responses and stress levels existed in either test attitude. A 50% run was also made in this attitude, followed by a 100% test run. The latter run never was completed due to structural damage encountered early in the test resulting from an inadvertent overloading of the test structure (control meter malfunction).

Repair of the damaged structure was effected; but, because of the structural changes, the remainder of the original test plan was cancelled. The vehicle was then utilized as a test bed for special vibration and acoustic studies.

In addition to presenting results on the various vibration tests, this report gives the results of two other activities, namely, the highway transportation by truck of a simulated SNAP structure mounted in a rocket sled and the sled test program conducted at the Edwards Air Force Base Experimental Track Branch at Edwards, California. This latter test program was developed to provide an acceleration test medium for the SNAP 10A-PSM-1 vehicle. With the vehicle damage incurred during vibration testing, however, no acceleration testing was performed on the PSM-1 unit. The sled test program was confined to two developmental runs employing a dummy test specimen.

II. SNAP 10A–PSM–1 VIBRATION TESTS

A. LATERAL FIRST BENDING AND DAMPING DETERMINATIONS

Before conducting any vibration tests on the shaker equipment, other tests to determine the lateral first fundamental bending frequency and the amount of structural damping were deemed necessary. To obtain this data, the S10A-PSM-1 test vehicle was firmly bolted to steel tiedowns embedded in concrete and the first fundamental mode was excited by applying a manual impulse near the center of gravity. Accelerometers mounted on the upper converter load ring and on the reactor top were monitored to obtain both the first resonant frequency and the vehicle response decay rate. From these tests it was determined that

$$f_n \approx 13.5 \text{ cps}$$

and

$$\text{structural damping} \approx 2\%.$$

Lateral (Y-Y) vibration testing later in the program showed that, with a more effective tiedown, $f_n \approx 17$ cps

B. VIBRATION TESTING – LONGITUDINAL AXIS (Z-Z)

Prior to making recorded test runs, low-level vibration surveys were made with the vehicle mounted on the upright shaker (Figure 1) in order to find vehicle resonances and to note whether any peculiar response conditions occurred which might require special attention or monitoring techniques during later tests. Generally, all low-level surveys were scanned at a constant octave sweep-rate from low to high frequency at a rate requiring ~11.5 min for a 5 to 3000-cps sweep. Vibration inputs to 3000 cps were ~10% of the specified vibration inputs. The 100% vibration levels are reproduced in Table 1 of this report. A deviation to these inputs was to be made at the first fundamental resonance in each axis with the table input being reduced so that the vehicle's center of gravity response would not exceed specified limitations (longitudinal : 2.5 g under 200 cps, lateral and normal: 2.0 g under 250 cps).

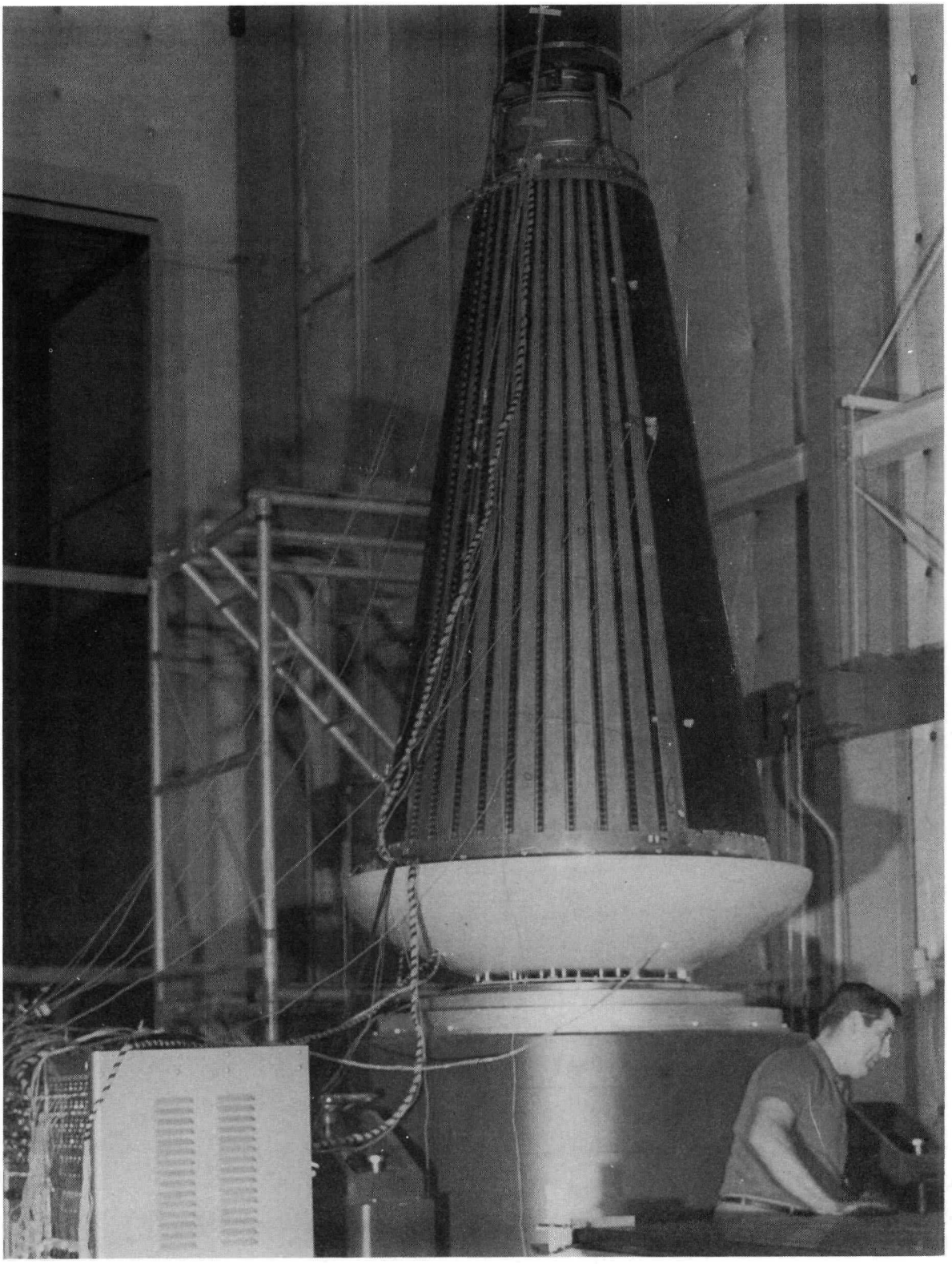

11-15-61 7580-5233

Figure 1. Specimen Installation on Upright 30,000-lb Shaker

TABLE 1

VIBRATION TEST INPUT LEVELS (100% VALUES)

Axis	Magnitude	Frequency (cps)
Longitudinal (Z-Z)	1/2 in. D.A.	5-9
	2.3 g	9-400
	7.5 g	400-3000
Lateral (Y-Y)	1/2 in. D.A.	5-8
Normal (X-X)	1.7 g	8-250
	4.5 g	250-400
	7.5 g	400-3000

Several vehicle locations were instrumented to be used as monitor points on all tests to follow. One sensor (126) was located on the base of the reactor can adjacent to the support leg on the -X axis. Another (7) was attached to the converter upper load ring on the -Y axis. The shield response was monitored by a pickup (131) located under the lower shield ring at a point adjacent to the shield support located midway between the +X and +Y axes. For all test runs in the longitudinal direction, the Z-Z component of acceleration at each of these three points was visually monitored so as not to exceed the 2.5 g acceleration restriction imposed by specification. In all vehicle acceleration surveys, all or part of these response points were recorded. Figure 2 notes the location of these and all other sensors employed during the vibration tests.*

Four vibration surveys followed in which outputs from all vehicle vibration sensors (accelerometers) were recorded. In all these runs, the first fundamental resonant frequency remained at 80 cps, with a fairly sharp 5 to 6 cps bandwidth. The only other resonance of appreciable interest occurred at ~400 cps. A modal vibration survey was not made at this frequency and so it was not determined exactly which resonance this was, i.e., second bending,

*For more details of locations or for sensors not noted on Figure 2, see Figure 42 at end of this report.

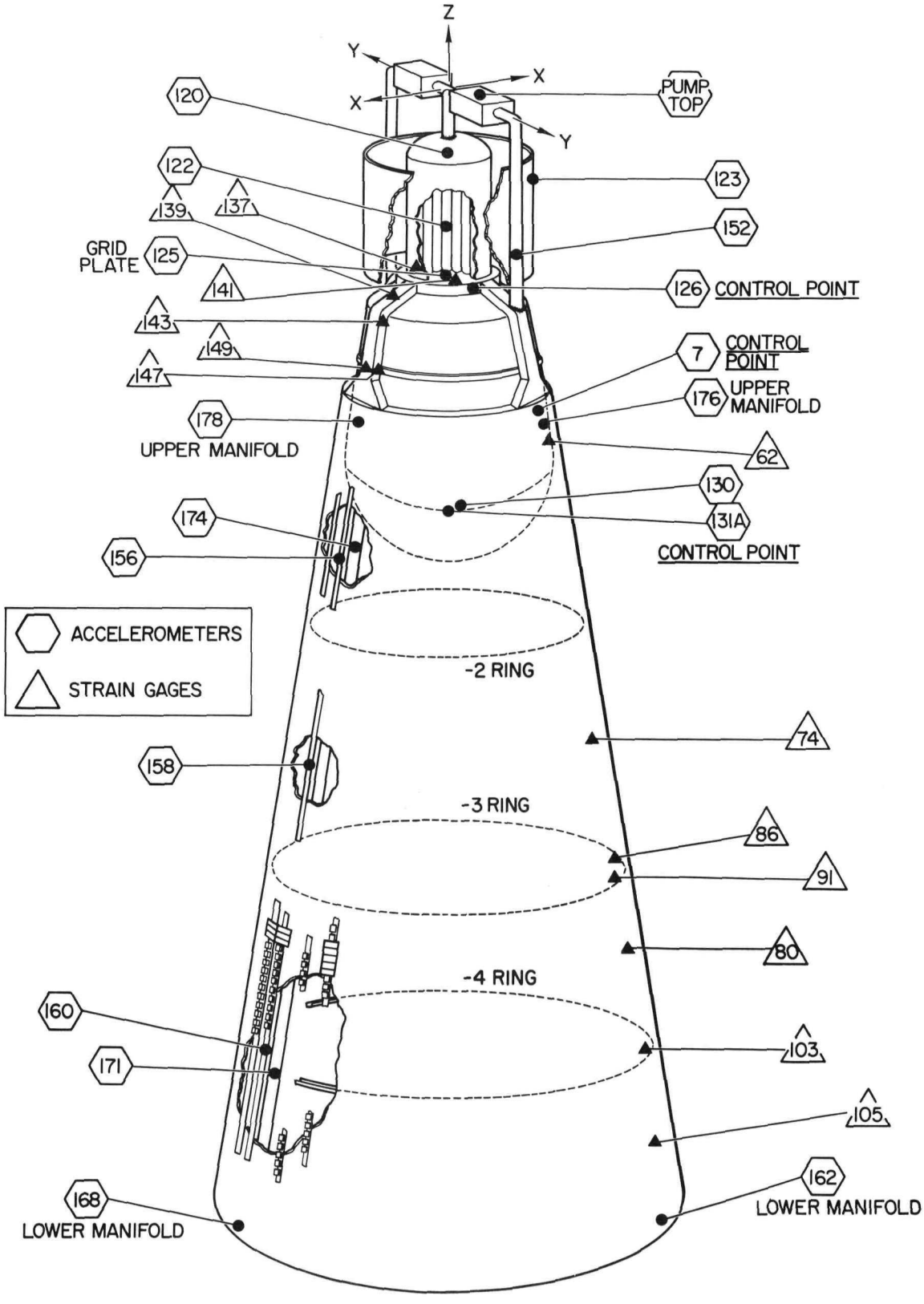

4-13-64

7561-01255

Figure 2. Accelerometer and Strain Gage Location

TABLE 2

LOW LEVEL SURVEY ACCELEROMETER RESPONSE – LONGITUDINAL (Z-Z)

Accelerometer Number	Location	Orientation	Magnification Factor			
			60* cps	70* cps	80† cps	400 cps
7	Converter upper load ring, outside	X-X	2.5	3	4, 6	3.9, 2.9
		Y-Y	2	5	5, 11	4.3, 3.0
		Z-Z	2.5	4	7, 10	2.7, 2.2
120	Reactor, top lid	X-X	0.5	1	6, 9, 16	0.6, 0.8, 0.6
		Z-Z	2	2.5	7.5, 21.5	1.1, 0.3
122	Center fuel element	Y-Y			6.5	
						2.2
123	Reflector, side	X-X	1	2	6.5	0.1
		Y-Y			2	0.3
		Z-Z			14	0.7
125	Lower grid plate	Z-Z			20	
						1.1
126	Reactor base, box ring	X-X	0.5	1	5, 8.5	0.7, 0.6
		Y-Y	1.5	2	1.5	0.2
		Z-Z	5	6	10.5, 11.5	
					13.5	0.9, 0.5
131	Shield, lower ring	tangent	2	2	2.5, 6	0.6, 1.3
		Z-Z	3	4.5	8, 10	1.0, 1.1
152	Supply line	X-X			13	3.3
		Y-Y			30.5	2.5
		Z-Z			11	4.1
157A	Converter tube	X-X			16.5	6.4
157B		X-X			26	7.5
157C		X-X			25	5.7
158A	Converter tube	X-X			18	7.1
158B		X-X			17	5.0
158C		X-X			17.5	7.2
160A	Converter tube	X-X	3	12.5	18	9.1
160C		X-X	3	6.5	25	6.0
172	Return Line	X-X	2	4.5	22, 24	2.1, 2.1
		Y-Y	2	5	12,13	8.1, 9.7
174	Return Line	X-X			16	5.7
		Y-Y			9.5	
						12.9

*Magnification factors at these frequencies are presented for comparison purposes.

†Multiple entries represent test scatter noted in the four acceleration runs.

third bending, torsional, etc. Table 2 explains the more important magnification factors observed on the test vehicle at ~80 and 400 cps.

Three points of particular interest are the main response control (monitor) points since they represent an approximation of the response at the center of gravity of the test vehicle. These values were extracted from Table 2 and are shown in Table 3. The magnification factors were calculated from the response measured at the first fundamental resonance with a 0.25 g table input.

TABLE 3

RESPONSE OF VEHICLE AT MONITOR POINTS

Sensor Location	Shaker Input (g)	Frequency (cps)	Magnification Factor (*)
7 (Z-Z)	0.25	80	7 to 10
126 (Z-Z)	0.25	80	10.5 to 13.5
131 (Z-Z)	0.25	80	8 to 10

*Test scatter noted in the four acceleration runs.

Following the acceleration surveys, strain data were recorded from five strain gage tests. Although visual monitoring of the outputs from accelerometers was maintained during these latter tests, no acceleration data were recorded. There was no indication of excessive strain at any of the gage locations. The first fundamental resonant frequency remained fixed; at no time did vehicle response at the particular monitor points exceed the 2.5 g limit values. Table 4 denotes all gage locations which indicated varying strains in excess of ±27μ in./in. (approximately 810 psi). These strains were maximum at approximately 80 cps. Negligible strains were recorded at all other frequencies for the table inputs applied.

It must be pointed out that, when referring to Table 2 for magnification factors, or to Table 4 for strain-gage data, that these values were obtained at a resonance where the vehicle's center-of-gravity response was limited to 2.5 g and where this limit was actually attained.

All nine runs previously noted were performed without water (to simulate NaK) in the system, so that later data could be compared with those from a system in which the damping effect of a fluid was present. This information,

TABLE 4

STRAIN GAGE DATA – LONGITUDINAL AXIS
AT 1st FUNDAMENTAL RESONANCE, 80 cps

Strain Gage Number	Strain Gage Location	Gage Orientation	Strain (μ in./in.)
62 A	Converter structure upper,	Z-Z	49
62 B	radial web, OD	*	27
80	Converter mid. -3, -4 ring, ID	Z-Z	46.5
86 A	Converter at -3 ring, ID	Z-Z	31
86 B		*	29.4
91 A	Converter at -3 ring, OD	Z-Z	30
94 A	Converter at -3 ring, ID	Z-Z	-
94 C		*	34
103 A	Converter structure lower, ID	Z-Z	-
103 C		*	27
105 A	Converter structure lower, radial web	Z-Z	47
139	Support leg, reactor vessel	Y-Y	95
141	Lower grid plate	Y-Y	64
143	Reactor leg	Z-Z	46
147	Reactor leg	Z-Z	34
149	Reactor leg	Z-Z	30

*Rosette gages are noted by identifying each individual leg as A, B, or C. Gage A is located in the direction of principal strain; gages B or C are located counterclockwise from A.

particularly that relating to the reactor vessel, was felt to be especially important. After the ninth test, the NaK system, complete except for the pump and two expansion compensators, was filled with 3-3/8 gal of water.

During the ensuing test run conducted to observe strain-gage outputs, a decided change in the first fundamental resonance was observed. Because of the magnitude of change, the addition of water proved to be coincidental and not the cause. Resonance now started at ~60 cps and continued to ~80 cps. The sudden change was traced to the shield, where an internal malfunction was suspected. Obviously a definite structural change had occurred, but the location and extent could not be ascertained from the information available from the strain gage data. Various accelerometer locations were checked in two additional runs. The same monitor points were carefully checked and the results noted in Table 5.

TABLE 5

RESPONSE OF VEHICLE AT MONITOR POINTS

Sensor Location	Shaker Input (g)	Frequency (cps)	Magnification factor*	
			Fundamental magnification factor	Total magnification factor
7 Z-Z (converter upper load ring)	0.12	60 to 70	8 to 11	8 to 11
126 Z-Z (reactor base)	0.12	60 to 70	9 to 16	9 to 16
131 Z-Z (shield lower ring)	0.12	60 to 70	14 to 30	17 to 60

*The total magnification factor includes the ringing which is superimposed on the fundamental response.

In comparing Table 5 with Table 3, it is immediately evident that the only appreciable change in vehicle response occurred on the sensor attached to the shield. At this point, the following possibilities presented themselves: (1) the bolts supporting the shield had loosened, (2) the shield support bracket on the converter shell had failed, (3) the accelerometer on the shield ring (131) was loose, (4) a crack in the lower shield ring (present before testing began) propagated, or (5) internal shield damage had occurred.

Visual inspection was performed and all shield support bolts were checked for tightness; none of the four main support bolts were loose. The accelerometer was still mounted rigidly and apparently in good working order. There was no indication of crack propagation in the shield ring, and no evidence of converter shield support bracket damage. Only internal shield damage could have caused the trouble.

The results of a run made with the instrumentation noted in Figure 3 are listed in Table 6. It should be noted that the 65 cps value was not the resonant frequency but a point within the general resonance range at which a clear relationship between the outputs from the various sensors could be obtained.

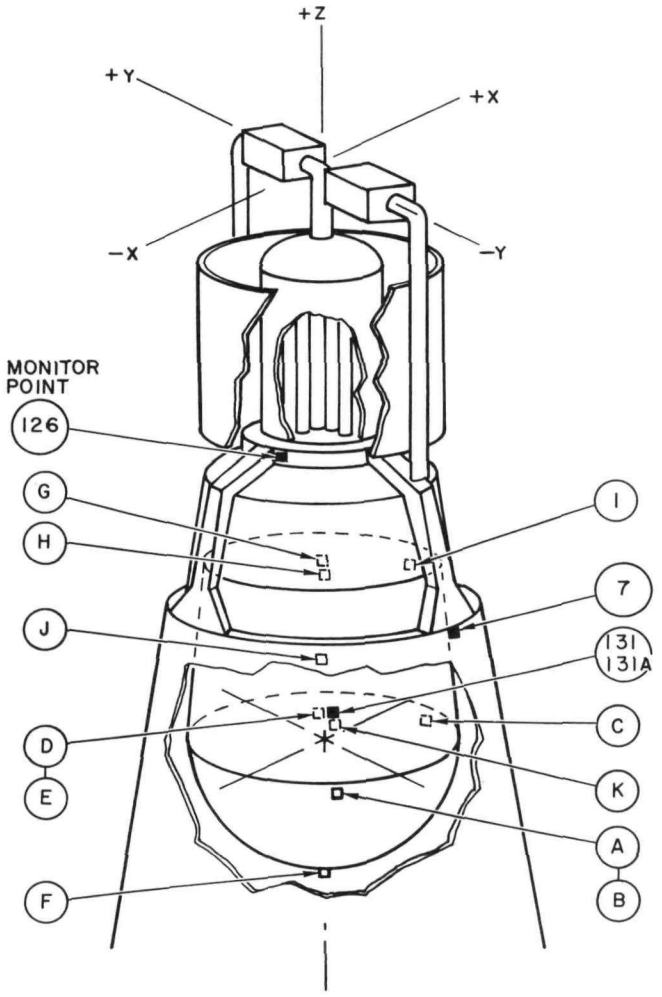

A. on shield lower ring between -X and -Y axes (tangent)

B. same as A, except for reading Z-Z

C. on shield lower ring, between +X and -Y axes (Z-Z)

D. on shield lower ring between +X and +Y axes (tangent)

E. same as D except for reading Z-Z direction

F. on shield bottom at shield centerline (Z-Z)

G. on shield, below midring between +X and +Y axes (Z-Z)

H. on converter upper load ring between +X and +Y axes (Z-Z)

I. on converter upper load ring between +X and -Y axes (Z-Z)

J. on converter upper load ring between -X and -Y axes (Z-Z)

K. 2 in. below 131, reading Z-Z

7. Monitor Point

131 Z-Z
131A. tangent

4-14-64 7561-01256

Figure 3. Accelerometer Locations Used During Shield Survey

Comparison of the results yielded the following observations:

1) The sensor outputs in the Z-Z direction of all three vehicle response locations were in the same order of magnitude prior to vehicle malfunction.

2) After the observed malfunction, the sensor output at the shield (131) increased from 1.5 to 5.5 times the values noted at the other locations.

3) During the shield survey run, a similar relationship between all shield lower ring response points and the sensors at locations 7 and 126 as noted in Item 2 above was obvious.

TABLE 6

SHIELD SURVEYS
(65 cps, 0.24 g Table Input)

Sensor Location	Sensor Orientation	Total Magnification Factor
A	Tangent to shield ring	Negligible
B	Z-Z axis	9
C	Z-Z axis	7
D	Tangent to shield ring	Negligible
E	Z-Z axis	4.5
F	Z-Z axis	3.5
G	Z-Z axis	2
H	Z-Z axis	Negligible
I	Z-Z axis	Negligible
J	Z-Z axis	2.5
K	Z-Z axis	6
7	X-X axis	Negligible
7	Z-Z axis	2
126	X-X axis	Negligible
126	Z-Z axis	2.5
131	Z-Z axis	4.5
131A	Tangent to shield ring	Negligible

While all sensors on the lower ring of the shield displayed readings of the same order of magnitude, these same readings were not in agreement with other locations observed on the shield. The effect of whatever malfunction had occurred, therefore, could be pinpointed to the general area of the shield lower ring. To get a better look at what was occurring at the lower ring locations, a run was made at high recorder speed for more efficient analysis of the output trace. It was observed that the fundamental response of the shield was still in good agreement with the reactor and converter shell response monitor points, 7 and 126. However, a 11,000 cps ringing was superimposed on the fundamental curve; the ringing pattern repeating itself on each cycle. Figure 4 reproduces a portion of the record showing the high-frequency shield-ring response.

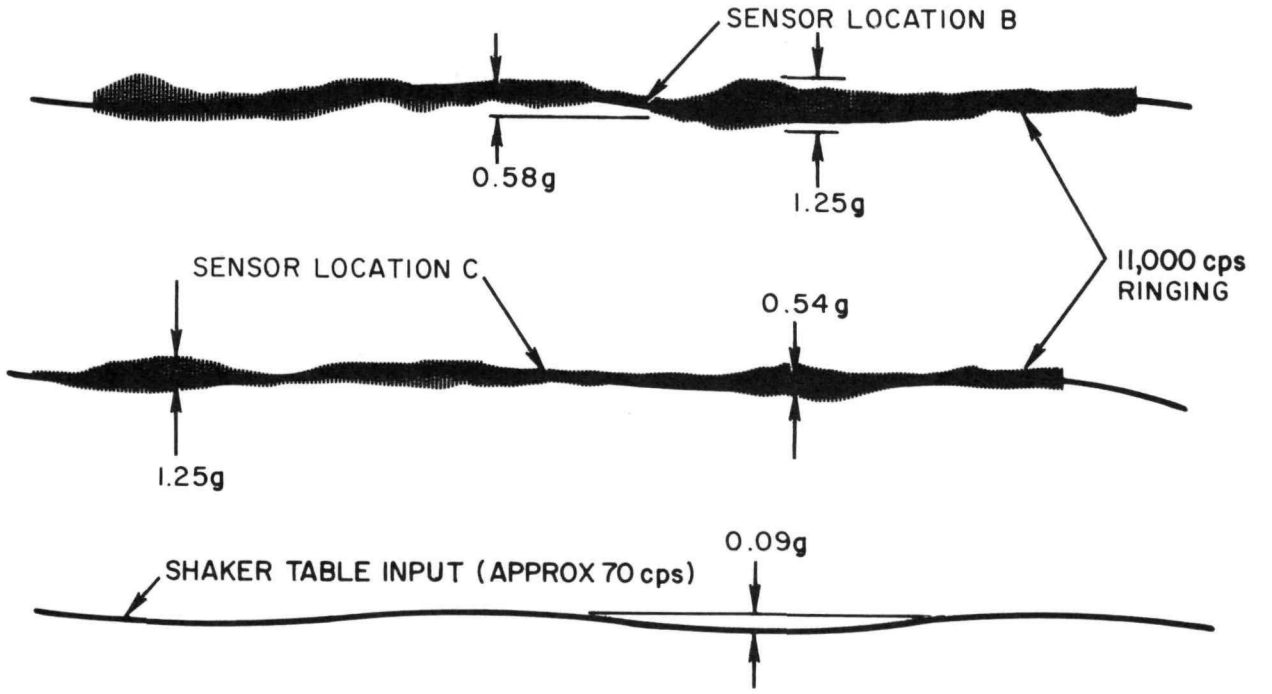

4-14-64 7561-01257

Figure 4. High Frequency Shield - Ring Response

Usually, the source of high-frequency response from low-frequency input, as noted on the shield, is the result of loose parts hammering or rattling in or on a structure. At this point in the test, it was deduced that somehow the lithium hydride mass in the shield had become loose and was bouncing on the steel support straps which in turn dumped the ringing response into the shield housing at the lower ring. Because internal shield damage was almost a certainty, the unit was replaced with a dummy. Prior to removal, one lateral test run was made on the vehicle to check the system for lateral first fundamental mode frequency and to gather data on magnification factors at various vehicle locations. The test was intended not to rule out the need for shield removal but rather to obtain the noted data with the actual shield still in place.

Subsequent X-ray examinations performed on the shield following removal from the vehicle revealed that:

1) In the upright position, cavitation of about one inch was found between the top of the shield containment vessel and the lithium hydride mass. X-ray disclosed that the internal mass had dropped approximately straight down.

2) X-rays were taken at 90° intervals perpendicular to the support ring in the areas of the lithium hydride support strap attachments. These shots revealed that the two positioning lug assemblies had become detached from the lug supports owing to failure of the welds.

3) The hydride mass was prevented from dropping to the bottom of the containment vessel by the remaining two positioning lugs that did not fail. Originally, cavitation was built into the hydride mass at these points to prevent complete slippage of the mass past this point, even though support failed on correspondingly opposite sides.

X-ray substantiated the fact that the support straps for the lithium hydride did not fail, but that failure had occurred at the weld between the positioning lugs and the shield containment vessel. Dissection of the shield several months later completely verified the X-ray diagnosis. Examination of the failure at that time revealed that the welds were little more than tack welds which were the result of the welder's inability to gain proper access to the weld area. This fact was instrumental in effecting a design change in the shield strap support system for all future shield assemblies.

Except at resonance (80 cps) where response limitations resulted in maximum inputs being applied to the vehicle, testing in the longitudinal axis was confined to low level survey investigations. It was intended that at the completion of low level testing in the other two axes a return to the longitudinal axis and higher input levels would be made.

A reasonable estimate of the total number of cycles imparted to the S10A-PSM-1 test vehicle during longitudinal testing is tabulated in Table 7. It must be remembered that these are only totals and can have fatigue significance only if corresponding stress levels can be determined. The most interesting bandwidth is the 70 to 80 cps range which includes ~15,000 cycles applied at the first fundamental resonance. Even though these latter cycles were at 100% of the specified values, their contribution to reduction of the structure's fatigue life was probably negligible. All stresses observed at resonance were <3000 psi; buckling of the corrugated shell was calculated to occur at about 14,000 psi.

TABLE 7

NUMBER OF CYCLES IMPARTED – LONGITUDINALLY

Frequency Range (cps)	Total Number of Cycles Applied (Approximate Values)	Comments
7-15	7,700	Table inputs were ~10% of the specification 100% values.
15-38	18,200	
38-50	11,200	
50-70	16,000	Table inputs were ~10% of the specification 100% values.
70-85	15,000	Magnification of input over this range (due to resonance) resulted in 100% loads to the structure.
85-100	25,600	Table inputs generally did not exceed 10% of the specification 100% values.
100-400	200,000	
400-500	64,000	
500-1000	336,000	
1000-2000	547,000	
2000-3000	220,000	Table inputs generally did not exceed 10% of the specification 100% values.
	Total 1,460,700	

C. VIBRATION TESTING – LATERAL AXIS (Y-Y)

Following the longitudinal test program, the PSM-1 unit was mounted on the slip table (Figure 5) and the vehicle was surveyed while lateral vibration

12-12-61 7580-5121

Figure 5. S10A-PSM-1 Vehicle Mounted on the Slip Table for Lateral Excitation

inputs were applied through the Y-Y axis. Two important resonances of basic vehicle structure were observed. The first fundamental resonance (1st bending) occurred at ~17 cps. A second significant resonance of unknown mode shape was observed at ~420 cps. In addition to these two, a converter tube bundle resonance occurred at ~42 cps. Preliminary test runs in this attitude were low-level surveys scanned at the same sweep rates followed in the longitudinal direction with test inputs of ~10 to 15% of the values noted in Table 1. An exception to this occurred at 15 to 18 cps (resonance) when the vehicle's center-of-gravity response points became the controlling factor. The monitor points depicted in Figure 3 were used as control locations, except that the Y-Y component of acceleration became the controlling signal and was restricted to 2 g below 250 cps.

Six low-level acceleration and three strain-gage test runs were conducted in the lateral attitude. Magnification factors and strain gage data obtained from these nine runs are compiled in Tables 8 through 12 and give values at the three prominent resonant conditions. Compared to these listed values, insignificant magnification factors and/or strain levels existed at all other frequencies in the test band at least for the shaker inputs applied.

During the converter tube bundle resonance at ~42 cps, excessive tube response and displacement was visually observed on some tubes, particularly on those near the vehicle X-X axis. On two separate tubes, double amplitudes (D.A.) of 1/16 in. were observed at converter midspan, with motion occurring sideways parallel to the support shell surface. This amplitude when related to shaker input represented a magnification factor of 60 and was well above those readings indicated during two separate runs by accelerometers mounted on the tube selected for instrumentation (Table 10).

The reason that such a large variation in tube response could occur on two tubes during the same test was due to the fact that three different NaK tube support clip configurations were being evaluated. Each type was to provide a "floating" spring-load design which would allow tube clip movement during thermal expansion and yet adequately constrain the tube under vibration, shock, and acceleration environments. Because the three clip designs did not possess the same spring rates, the resonant frequencies of the tubes held by the clips varied from tube to tube. The resonant frequency of the tube with high amplification coincided with the resonant frequency of the entire tube bundle

TABLE 8

ACCELEROMETER RESPONSE – LATERAL (Y-Y) AXIS
AT 1st FUNDAMENTAL RESONANCE ≈17 cps

Accelerometer Number	Location	Orientation	Total Magnification Factor	Fundamental Magnification Factor
7	Converter upper ring, outside	X-X Y-Y Z-Z	7, 6, 6.8, 6 33, 30, 22.7, 36 10	3, 3, 4.2, 6 25, 20, 14.3, 27 10
126	Reactor base, box ring	X-X Y-Y Z-Z	6 25, 21, 15.5, 30 -	6 25, 21, 15.5, 30 -
131	Shield, lower ring	Y-Y Z-Z	23, 26, 18.2 4, 3, 1.7, 3	23, 18, 12.5 4, 3, 1.7, 3
156B	Converter tube	X-X	10.5	6.5
156C	Converter tube	X-X	7.7	5.5
158A	Converter tube	X-X Y-Y	12.2 15	8.6 11
158B	Converter tube	X-X Y-Y	6.4 17	4.8 8
158C	Converter tube	X-X Y-Y	4.5 17	4.5 9
160A	Converter tube	X-X	9.3	5.1
160C	Converter tube	X-X	6.8, 15	5, 15
171	Return line	X-X	25	15
174	Return line	X-X Y-Y	17 15	6 15
122	Center fuel element	Y-Y	17	17
152	Supply line	Y-Y	26	26
	Pump top	X-X Y-Y	3 29	3 29
Dummy Shield Instrumentation	Shield ring 180° from 131	Y-Y	23	23
	Shield lower face on vehicle centerline	Y-Y	20	20
	On the side of shield below the center ring and between -X, -Y axes	Y-Y	22	22
	Upper converter load ring between +X, -Y axes	Y-Y	22	22
	Upper converter load ring between -X, -Y axes	Y-Y	21	21
162	Bottom manifold	X-X Y-Y	3 4	
168	Bottom manifold	Y-Y	3	
176	Top manifold	Y-Y	117	
178	Top manifold	X-X	53	

TABLE 9

STRAIN GAGE DATA – LATERAL (Y-Y) AXIS
AT 1st FUNDAMENTAL RESONANCE ≈ 17 cps

Gage Number	Location	Gage Orientation	Strain (μ in./in.)
2A	Upper ring, outside	Z-Z	20.8
2B		*	81.5
2C		*	78
6	Upper ring, inner top flange	45° to X-Y	22.5
11	Upper ring, inner bottom flange	45° to X-Y	35.7
15	Shield support flange	Z-Z	20.8
21	Upper ring, Z, outer flange	45° to X-Y	64.2
22	Upper ring, Z, inner flange	45° to X-Y	9.3
25A	Upper ring, Z web	45° to X-Y	50.6
25B		*	59
25C		*	37.2
27A	Upper torque box	20° from X-X	-
27B		*	73
27C		*	18.2
33A	Lower ring, inner	Z-Z	37
33B		*	31.5
33C		*	17.6
54	10L136-62001-4 ring, inner flange	X-X	25.5
62A	Converter structure upper, OD radial web	Z-Z	150
62B		*	78.2
62C		*	39.1
65A	Converter structure upper, ID	Z-Z	86.6
65B		*	53
65C		*	15
74	Converter mid-2, -3 ID	Z-Z	156
80	Converter mid -3, -4 ring, ID	Z-Z	208
86A	Converter at -3 ring, ID	Z-Z	202
86B		*	178
86C		*	96

*Rosette gages are noted by identifying each individual leg as A, B, or C. Gage A is located in the direction of principal strain; gages B or C are located counterclockwise from A.

TABLE 9 (Continued)

Gage Number	Location	Gage Orientation	Strain (μ in./in.)
88A	Converter at -3 ring, radial web	Z-Z	230
88B		*	83
88C		*	10.4
91A	Converter at -3 ring, OD	Z-Z	-
91B		*	160
91C		*	89.5
94A	Converter at -3 ring, ID	Z-Z	15.5
94B		*	31
94C		*	34.6
103A	Converter structure, lower ID	Z-Z	32
103B		*	53.7
103C		*	68.8
105A	Converter structure, lower radial web	Z-Z	124
105B		*	63
105C		*	28.3
106A	Converter structure, lower OD	Z-Z	76.2
106B		*	27.5
106C		*	30
132	Reactor top	Y-Y	18.4
133	Upper grid	Y-Y	11.3
135	Vessel	Z-Z	-
137	Vessel	Z-Z	29.2
139	Support leg	Y-Y	41
141	Lower grid	Y-Y	-
143	Leg	Z-Z	3.7
145	Leg	Z-Z	7.4
147	Leg	Z-Z	60
149	Leg	Z-Z	51

*Rosette gages are noted by identifying each individual leg as A, B, or C. Gage A is located in the direction of principal strain; gages B or C are located counterclockwise from A.

TABLE 10

ACCELEROMETER RESPONSE – LATERAL (Y-Y) ≈ 42 cps
LOW LEVEL INPUT

Accelerometer Number	Location	Orientation	Total Magnification Factor	Fundamental Magnification Factor
7	Converter, upper load ring outside	X-X Y-Y	0.9, 2.3, 4.4 2.6, 3.5, 9	0.9, 2.3, 1.5 2.6, 3.5, 2.2
120	Reactor, top surface	Y-Y	3.4	3.4
126	Reactor base, box ring	X-X Y-Y	0.8 0.5, 0.8	0.8 0.5, 0.8
131A	Shield, lower ring	Y-Y	1.6, 2.1, 4	1.6, 2.1, 4
131	Shield, lower ring	Z-Z	0.7, 1.1, 0.8	0.7, 1.1, 0.8
156A	Converter tube	X-X	4.8, 16	4.8, 13
156B	Converter tube	X-X	11.5, 0.6	11.5, 0.5
156C	Converter tube	X-X	7.6, 17	7.6, 14.2
158A	Converter tube	Y-Y	4	4
158B	Converter tube	X-X	7.4, 18.3	7.4, 18.3
158C	Converter tube	Y-Y	9, 5.2	9, 5.2
160A	Converter tube	X-X	9.4, 0.26	9.4, 0.17
160C	Converter tube	X-X	8, 26	8, 12.4
162	Bottom manifold	X-X Y-Y	11.4 21	11.4 21
168	Bottom manifold	X-X Y-Y Z-Z	20 8.7 13.6	20 8.7 13.6
176	Upper manifold	Y-Y	18	18
178	Upper manifold	X-X	15	15
	Pump	Y-Y	0.8	0.7

TABLE 11

STRAIN GAGE DATA – LATERAL (Y-Y), 42 cps
LOW LEVEL INPUT

Strain Gage Number	Location	Gage Orientation	Strain (μ in./in.)
25 A	Upper ring Z web	45° to X-Y	11
B	Upper ring Z web	*	10
C	Upper ring Z web	*	29
65 A	Converter structure upper, ID	Z-Z	-
B		*	5
C		*	15
74	Converter mid. -2, -3 ID	Z-Z	16
80	Converter mid. -3, -4 ring,ID	Z-Z	16
86 A	Converter at -3 ring, ID	Z-Z	22
B		*	20
C		*	30
91 A	Converter at -3 ring, OD	Z-Z	-
B		*	18
94 A	Converter at -3 ring, ID	Z-Z	-
B		*	30
C		*	22
103 A	Converter structure lower, ID	Z-Z	16
B		*	11
C		*	13
105 A	Converter structure lower	Z-Z	32
B	radial web	*	21
C		*	13
106 A	Converter structure lower OD	Z-Z	17
B		*	14
C		*	13
139	Support leg	Y-Y	18

*Rosette gages are noted by identifying each individual leg as A, B, C. Gage A is located in the direction of principal strain; gages B or C are located counter-clockwise from A.

TABLE 12

ACCELEROMETER DATA – LATERAL (Y-Y), 420 cps
LOW LEVEL INPUT

Accelerometer Number	Location	Orientation	Total Magnification Factor	Fundamental Magnification Factor
7	Converter upper load ring outside	X-X Y-Y	1, 0.8, 0.6 2.7, 3.7, 3.9	1, 0.8, 0.6 2.7, 3.7, 2.5
131 131A	Lower shield ring	Z-Z Y-Y	0.2, 0.2 0.7, 0.3, 0.8	0.2, 0.2 0.7, 0.3, 0.8
156A	Converter tube	Y-Y	10	10
B		Y-Y	3.5	3.5
C		X-X	1.6, 1.0	1.6, 1.0
158A	Converter tube	Y-Y	7.5, 1.4	7.5, 1.4
B		Y-Y	9.2, 1.4	9.2, 1.0
C		X-X	4.3, 2.1	4.3, 2.1
160A	Converter tube	X-X	1.0	0.7
C		X-X	0.8, 2	0.8, 2
168	Bottom manifold	Z-Z	4.5	4.5
171	Return line	X-X	1.6	1.6
174B	Return line	X-X	1.1	1.1

and thus gave rise to the high value. None of the three clip designs was found to be a completely satisfactory support device and so a redesign of tube support for future vehicles was started by the Project. Because this test program obsoleted the existing attachments, a discussion of their design is not included in this report.

The large response on some tubes was not without damage. In the course of these tests, four tube support clips separated from the converter tube due to braze failures. The attachment bolt on one additional clip became loose, and in several instances, simulated radiators fell off.

Excessive displacement was not confined to the converter tubes. The upper and lower manifolds also experienced large motion. The confined

manifolds were limited in travel to the internal clearance existing in the converter shell upper and lower load rings. During vibration when this clearance was not adequate to prevent manifold-converter shell contact, high-frequency ringing was generated on the output of any and all sensors located in the vicinity.

Magnification factors at 42 cps are noted in Table 10 and give values measured in the X-X, Y-Y direction at various converter tube locations. At this frequency, the Z-Z component of acceleration was not significant. At 17 cps, however, the Z-Z motion of the lower manifold, which measured 1/32 in. D.A., had an extreme effect on manifold magnification factors (Table 8). The high magnification factors at 17 cps resulted when the entire tube bundle rocked out of phase with the basic PSM-1 structure; because of sufficient amplitude, the manifolds hammered against the shell structure causing high g-loads and the resulting large magnification factors at those points.

In spite of the adverse response of the converter tube structure, no damage to the tubes or manifolds could be observed. Since the system was filled with water, a leak would be the obvious means of detecting damage; none was found.

After completion of the low-level runs, a 50% lateral test using eighteen accelerometers and fifteen strain gages was conducted. The choice of sensor locations was dictated by the results of previous low-level runs. This run was scanned at the same sweep rate as before and the same response control points and response limitations were in effect. Tables 13 and 14 list the acceleration response and strain levels that existed at 17 and 42 cps during this run.

The only damage observed was confined to converter tube support clips. Four braze failures were noted, one clip became unbolted, and one radiator and simulated converter pellet fell off. No other damage could be found.

Table 15 presents a reasonable estimate of the total number of cycles applied at low level and at 50% of the specification values to the S10A-PSM-1 test vehicle during the lateral test series. In considering the cycles at 15 to 17 cps, all were applied at 100% specification values. As related previously, other totals can have fatigue significance only if stress levels can be determined.

TABLE 13

ACCELEROMETER RESPONSE – LATERAL (Y-Y) AXIS, 50% RUN

Accelerometer Number	Location	Orientation	Total Magnification Factor / Fundamental Magnification Factor	
			17 cps	42 cps
7	Converter upper ring, outside	X-X	2.6 / 2.6	1.5 / 0.8
		Y-Y	21.6 / 16	4 / 2
		Z-Z	4.6 / 4.6	0.9 / 0.9
120	Reactor, top surface	X-X	27.2 / 27.2	0.3 / 0.3
		Y-Y	23.2 / 23.2	1.3 / 1.3
122	Center fuel element	Y-Y	22.4 / 22.4	0.6 / 0.6
123	Reflector, side	Y-Y	19.2 / 19.2	1 / 1
126	Reactor base, box ring	X-X	5 / 5	Negligible
		Y-Y	19.2 / 19.2	0.4 / 0.4
131	Lower shield ring	Y-Y	16.8 / 16.8	1.4 / 0.9
		Z-Z	2.3 / 2.3	0.5 / 0.5
156 A	Converter tube	Y-Y	13.6 / 13.6	6.6 / 4
156 B	Converter tube	Y-Y	8 / 8	9.3 / 6.5
158 A	Converter tube	Y-Y	19.2 / 12	3.5 / 3.5
	Pump	Y-Y	24 / 24	1.9 / 1.9

TABLE 14

STRAIN GAGE DATA – LATERAL (Y-Y) AXIS, 50% RUN

Gage Number	Location	Gage Orientation	Strain (μ in./in.)	
			17 cps	42 cps
2 A	Upper ring, outside	Z-Z	-	-
2 B		*	132	36
62 A	Converter structure upper,	Z-Z	159	43
B	OD radial web	*	93	20
65 A	Converter structure upper ID	Z-Z	66	12
74	Converter mid. -2, -3 ID	Z-Z	180	5.5
80	Converter mid. -3, -4 ring, ID	Z-Z	246	43.5
86 A	Converter at -3 ring ID	Z-Z	230	32.7
B		*	216	72
C		*	112	30.5
88 A	Converter at -3 ring	Z-Z	284	21.8
B	radial web	*	115	12.8
91 A	Converter at -3 ring OD	Z-Z	-	-
B		*	176	29.4
C		*	100	10
105 A	Converter structure lower radial web	Z-Z	375	6.8
106 A	Converter structure lower OD	Z-Z	188	31.4

*Rosette gages are noted by identifying each individual leg as A, B, or C. Gage A is located in the direction of principal strain; gages B and C are located counterclockwise from A.

TABLE 15

NUMBER OF CYCLES IMPARTED – LATERALLY, Y-Y AXIS

Frequency Range (cps)	Total Number of Cycles Applied		Comments
	At Approximately 10% of Specified Values	At Approximately 50% of Specified Values	
7-15	12,100	1,100	
15-17	3,600	300	Magnification of input over this range (due to resonance) resulted in 100% loads to the structure
17-38	24,000	2,400	
38-50	16,600	1,600	
50-70	20,000	2,000	
70-100	32,000	3,200	
100-400	250,000	25,000	
400-500	96,000	8,000	
500-1000	462,000	42,000	
1000-2000	168,400	84,200	
2000-3000	-	81,800	
Total	1,084,700	251,600	
Grand Total	1,336,300		

D. VIBRATION TESTING – NORMAL AXIS (X-X)

After the 50% lateral test run was completed, the PSM-1 test vehicle was rotated 90° on the slip table so that vibration tests could be conducted through the third and final axis. Because the vehicle is essentially symmetrical about either the lateral (Y-Y) axis or the normal (X-X) axis, only one low-level test run was conducted to establish that similar vehicle responses and stress levels existed in either test attitude. The results of the test run verified this fact. This low-level run employed sweep rates, table inputs, and response controls similar to those followed in the lateral low-level series.

A 50% test run in the normal attitude followed the single low-level sweep. Tables 16 and 17 indicate the magnification factors and strains observed at the two most important resonant conditions, 17 and 42 cps. The similarity of vehicle response for related locations can be readily seen by comparison with the lateral 50% run.

During the 50% test run, seven more converter tube clips experienced tube-to-clip braze failures. No other vehicle damage was observed. Nothing on the test record indicated any cause for concern in making a 100% run as long as proper vehicle response monitoring was maintained over the frequency range specified.

Using the same sensor locations as in the 50% run and the same monitoring locations and techniques, a 100% run was started. Because the first fundamental natural frequency of the 30,000-lb vibration shaker and the large slip table as a combined system occurs between 7 and 10 cps, testing in the normal attitude was started at 12 cps and scanned at a constant octave sweep rate, which normally would require 25 min for a 5 to 3000-cps sweep. At 38 cps or 5.2 min later, testing was stopped and damage noted. Severe buckling of all converter shell corrugations had occurred near the base of the shell structure and the damage was too extensive to permit continuation of testing Figures (6, 7, and 8).

Testing was stopped at 38 cps, not because damage had been detected, but because the instrument being used to record test results had run out of paper. Until this occurred, there had been no indication of vehicle failure, at least visually. Evaluation of the test record revealed that vehicle center of gravity response limitations had been exceeded. The inadvertent overloading

TABLE 16

ACCELEROMETER RESPONSE – NORMAL (X-X) AXIS, 50% RUN

Accelerometer Number	Location	Orientation	Total Magnification Factor / Fundamental Magnification Factor	
			17 cps	42 cps
7	Converter upper ring, outside	X-X	18.2 / 16.4	1.8 / 1.1
		Y-Y	8.9 / 4.2	3.2 / 1.6
		Z-Z	0.9 / 0.9	1.2 / 0.8
120	Reactor, top surface	X-X Y-Y	2.0 3.8	1.7 0.3
122	Center fuel element	Y-Y	-	-
123	Reflector, side	Y-Y	-	-
126	Reactor base, box ring	X-X Y-Y	11.7 10	0.8 0.3
131	Lower shield ring	Y-Y Z-Z	3.3 2.7	0.9 0.2
156 A	Converter tube	Y-Y	15.7 / 7.9	7.6 / 2.1
156 B	Converter tube	Y-Y	-	8.8 / 3.7
158 A	Converter tube	Y-Y	13.6 / 6.8	8.1 / 6.2
	Pump	Y-Y	-	0.7
174 B	Return line	X-X	48 / 26.6	15.6 (noise)
125	Grid plate	Z-Z	1.4	0.2

TABLE 17

STRAIN GAGE DATA, NORMAL (X-X) AXIS, 50% RUN

Gage Number	Location	Gage Orientation	Strain (μ in./in.)	
			17 cps	42 cps
2A	Upper ring, outside	Z-Z	-	-
2B		*	24	-
62A	Converter structure upper OD	Z-Z	24	12
62B	radial web	*	18	6
65A	Converter structure upper ID	Z-Z	24	12
74	Converter mid -2, -3 ID	Z-Z	10.8	5.4
80	Converter mid -3, -4 ring ID	Z-Z	10.8	24
86A	Converter at -3 ring ID	Z-Z	10.8	16.2
86B		*	24	18
86C		*	9.6	24
88A	Converter at -3 ring radial web	Z-Z	5.4	10.8
88B		*	6	84
91A	Converter at -3 ring OD	Z-Z	-	-
91B		*	54	23.4
91C		*	4.8	9.6
105A	Converter structure lower radial web	Z-Z	6	26.4
106A	Converter structure lower OD	Z-Z	4.2	8.4

*Rosette gages are noted by identifying each individual leg as A, B, or C. Gage A is located in the direction of principal strain; gages B or C are located counterclockwise from A.

of the test specimen was traced to the meter used for visually monitoring the most important response location, (No. 7) noted on Figure 3. During testing, this meter failed to give a reading. It was discovered that a small piece of metal casting had fallen into the meter needle mechanism preventing needle motion. The metal particle inside the meter case had been overlooked by the manufacturer.

Initial failure started exactly 5 sec after the data recording device was turned on. The recorder was started when the input to the vehicle base ring

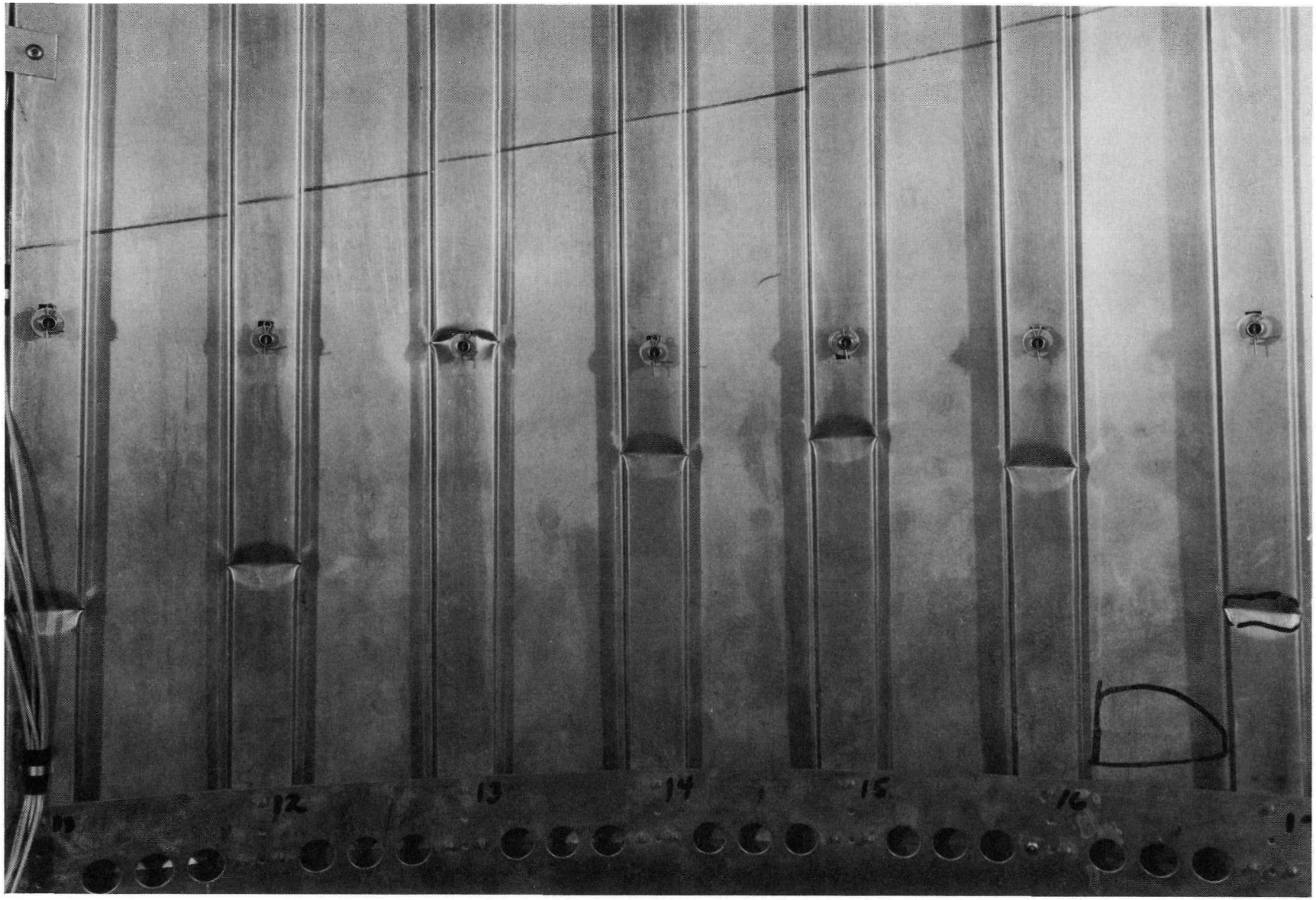

12-26-61

7580-5126G

Figure 6. Damaged Converter Structure (Part 1)

12-26-61

7580-5126H

Figure 7. Damaged Converter Structure (Part 2)

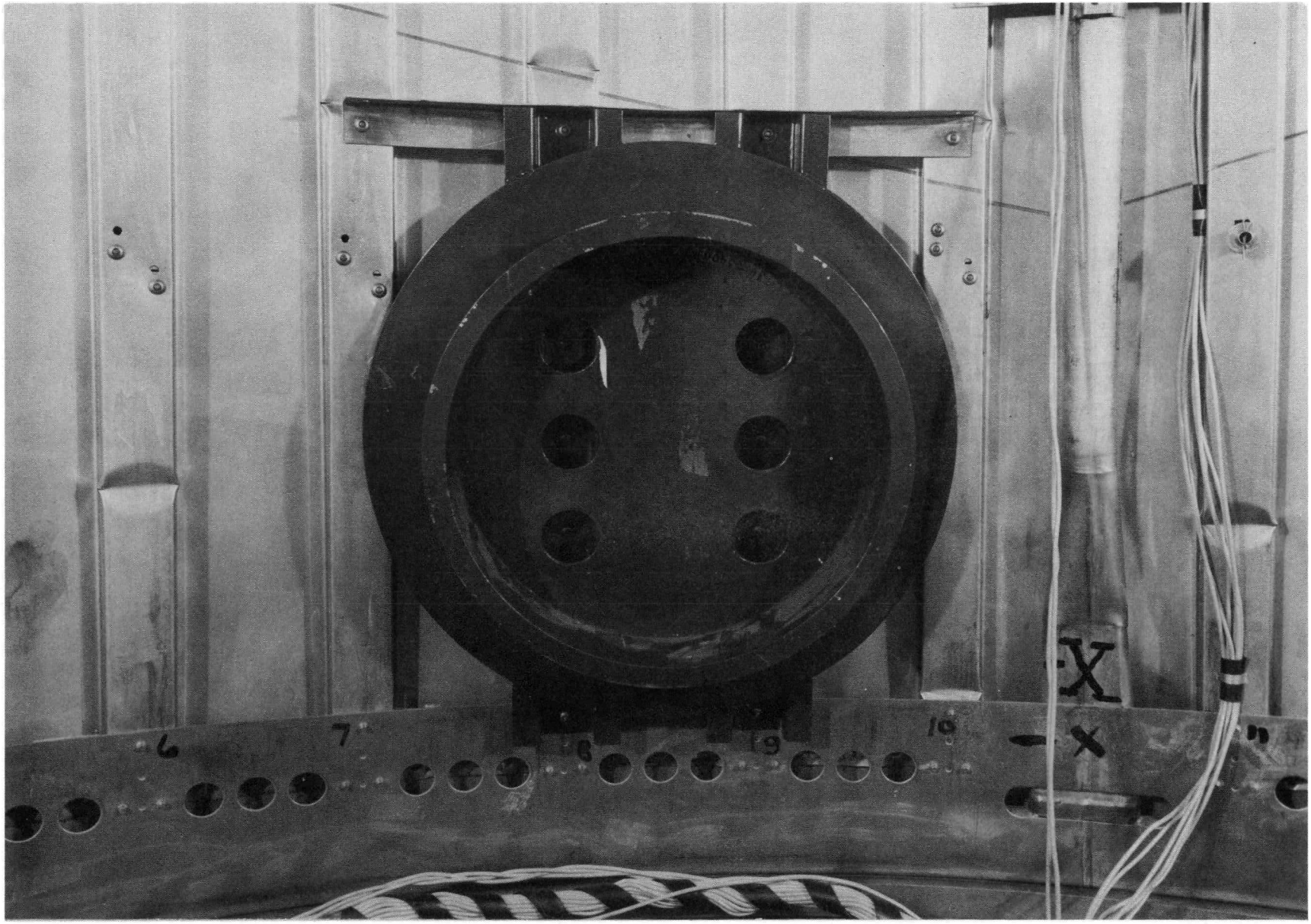

12-26-61

7580-5126F

Figure 8. Damaged Converter Structure (Part 3)
(Note damage at top of expansion compensator mockup)

reached 1.33 g at a frequency of ~12 cps, and 60 cycles later the test recorder indicated an occurring failure. Figure 9 reproduces the test run record during structural failure. At 60 cycles discontinuities appeared on most traces and indicated structural damage. The resulting damage was sufficient to drop the vehicle's first fundamental natural frequency from 17 to 12 cps. The upsurge in table input was caused by the fairly constant table input suddenly applied at this new resonance. The equally abrupt drop-off of both table input and vehicle response after resonance was due to rapid passing out of resonance (<4 cycles). Table 18 presents fundamental magnification values at the start of test recording and at various noted points before, during, and after failure. Ringing on various traces is not included in the values shown in the table; their contribution to the total trace can be seen in Figure 9. Table 19 tabulates strain gage data for the test run.

It is believed that initial shell damage started in the corrugations to one side of the X-X axis and on both sides of the vehicle directly above the expansion compensator mockups. The compensator mockups consisted of very stiff masses tightly attached to four corrugations on each side of the vehicle. Being quite rigid, the simulated units carried the bulk of the load in the region of the highly stressed X-X axis. These in turn dumped the load into the four corrugations at a point ~1 ft above the base ring. Since the corrugations were subjected to more than a fair share of the load, structural buckling resulted directly above the compensator mockup, Figure 8. When these four corrugations on each side of the vehicle failed, the remaining structure had to carry the load. With the overload conditions, all remaining corrugations buckled in the general region of the base ring. Repeated testing after initial failure only served to increase the severity of damage on each corrugation. It can be speculated that the converter shell might have actually withstood the overload conditions if the stress raiser imposed by the compensator mockup had not been present.

While the overloading that caused the PSM-1 vehicle structural failure was not purposely planned, it did provide valuable information for future structures. The awareness of and the need to eliminate stress raisers such as the compensator mockup type of installation was of great significance. Paralleling this requirement was the necessity of a base ring design that would permit gradual and uniform transition of load from the base ring to the shell structure.

TABLE 18

ACCELEROMETER RESPONSE – NORMAL (X-X) AXIS, 100% TEST RUN, 12 cps

Accelerometer Number	Location	Orientation	Fundamental Magnification Factor (at the cycle noted, see Figure 9)									
			Start	30	58	59	60	61	62	63	64	65
	Table input	X-X	1.3g	1.3g	1.1g	1.1g	1.1g	1.3g	1.8g	1.4g	0.9g	0.6g
7	Converter, upper ring, outside	X-X	2.5	2.6	3.8	3.9	3.5	3.4	2	1.9	2.3	2.4
		Y-Y	0.5	0.7	0.9	0.8	0.8	0.5	0.4	0.3	0.4	0.3
		Z-Z	0.1	0.2	0.3	0.3	0.5	0.7	0.6	1	0.9	0.6
120	Reactor, top surface	X-X	2.4	4.2	6	6	6	5.3	3.7	3.8	4	4.8
		Y-Y	-	-	-	0.2	0.5	0.5	0.2	0.2	0.2	0.3
123	Reflector, side	Y-Y	-	-	-	0.2	0.2	0.3	0.3	0.3	0.5	0.3
126	Reactor base, box ring	X-X	1.7	2.1	3	3.4	3.4	3	2.2	2.1	2.6	2.6
		Y-Y	1.3	1.5	2.1	2.3	2.3	1.7	1.2	1.2	1.6	1.7
131	Lower shield ring	Y-Y	0.1	Noise →								
		Z-Z	0.4	0.6	0.9	1	1	1.1	1.2	1.2	0.9	0.9
156 D	Converter tube	Y-Y	2	2.4	3.2	2.9	3	2.7	1.6	1.2	1.2	1.2
158 D	Converter tube	Y-Y	1.3	1.7	3	3.3	3	3.5	1.6	2.5	4.4	3.5
160 D	Converter tube	Y-Y	1.3	1.8	2	2	1.7	1.5	1.3	1.6	4.6	2.3
	Pump	Y-Y	-	-	-	0.5	0.5	0.5	0.5	0.5	0.3	0.9
125	Grid plate	Z-Z	-	-	0.3	0.5	0.7	1	0.8	1	0.8	0.9
174 B	Return line	X-X	2.2	3.4	4	4.8	4.1	3.8	2.7	2.1	3.4	3.6

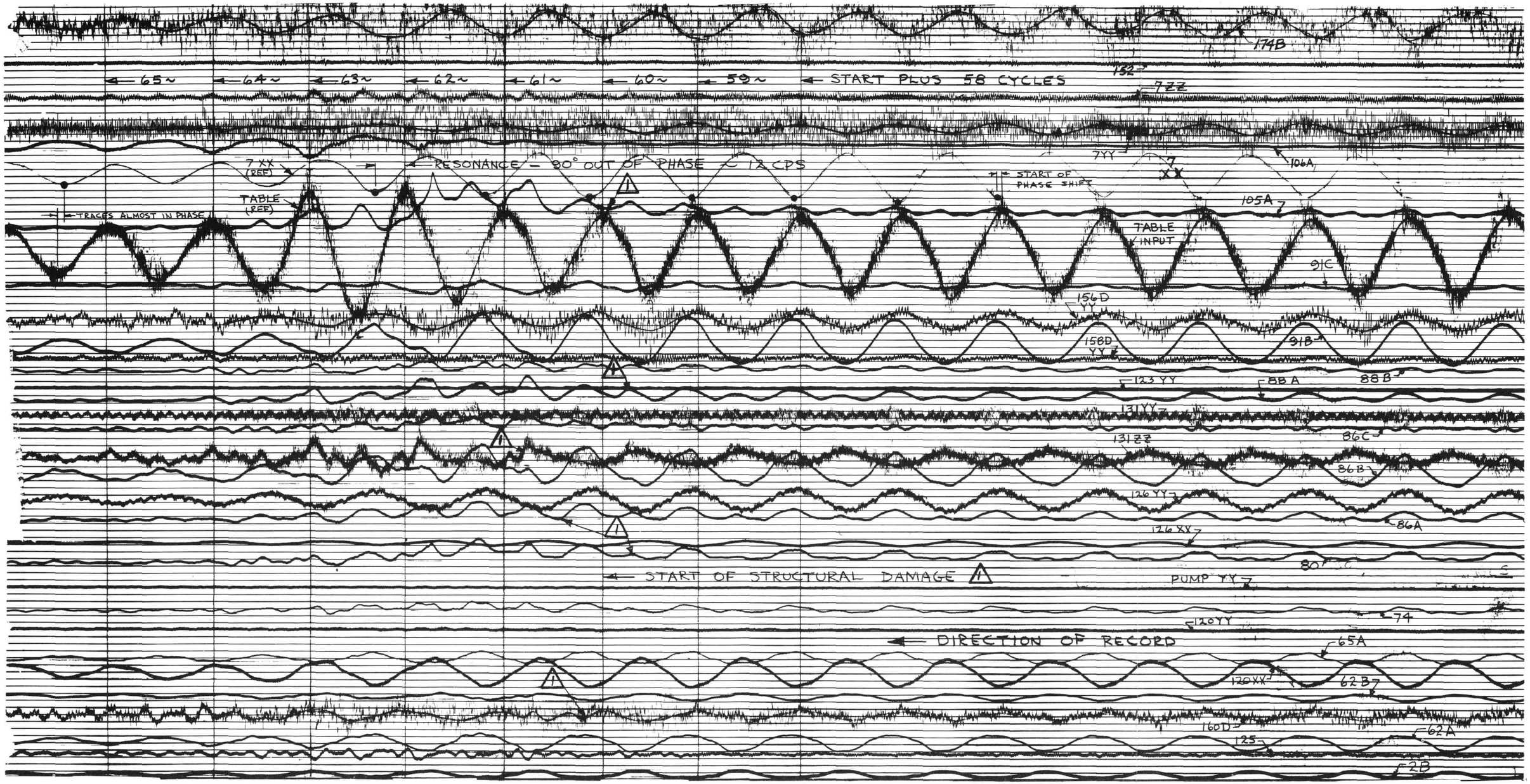

4-15-64 7561-01258

Figure 9. Oscillogram Record of S10A-PSM-1 Failure

BLANK

TABLE 19

STRAIN GAGE DATA – NORMAL (X-X) AXIS, 100% TEST RUN, 12 cps

Gage Number	Location	Gage Orientation	Strain (μ in./in. at the cycle noted, see Figure 9)									
			Start	30	58	59	60	61	62	63	64	65
2 A	Upper ring OD	Z-Z	-	-	-	-	-	-	-	-	-	-
B		*	50	50	63	63	63	63	63	50	38	25
62 A	Converter structure, upper, OD radial web	Z-Z	88	100	138	138	150	163	138	100	75	63
B		*	70	70	70	70	70	70	70	70	42	42
65 A	Converter structure, upper ID	Z-Z	60	72	96	96	96	96	84	60	48	36
74	Converter mid -2, -3 ID	Z-Z	26	38	64	64	89	64	64	77	38	26
80	Converter mid -2, -4 ring, ID	Z-Z	38	51	115	115	128	128	153	89	51	25
86 A	Converter at -3 ring, ID	Z-Z	38	51	102	102	140	115	115	77	51	38
B		*	145	165	259	269	290	279	197	134	93	83
C		*	20	20	39	49	49	79	98	59	39	20
88 A	Converter at -3 ring, radial web	Z-Z	30	30	80	90	90	170	150	110	40	20
B		*	20	20	30	40	50	70	70	60	40	30
91 A	Converter at -3 ring, OD	Z-Z	-	-	-	-	-	-	-	-	-	-
B		*	231	277	381	381	381	450	289	196	127	104
C		*	20	30	50	70	80	100	80	50	30	20
105 A	Converter structure, lower radial web	Z-Z	13	13	93	107	133	320	533	160	80	40
106 A	Converter structure lower OD	Z-Z	19	19	38	38	38	38	169	225	169	132

*Rosette gages are noted by identifying each individual leg as A, B, or C. Gage A is located in the direction of principal strain; gages B or C are located counterclockwise from A.

Lack of this necessity in the PSM-1 design was evident directly adjacent to the base ring in the flat panels between corrugations. Buckling of the flat plates occurred because a rivet in the load ring dumped excessive load into this essentially nonstructural member. While the particular damage was minor, the fact that it occurred should be borne in mind in future designs.

The damaged structure was repaired so that it could still be used as a test bed for subsequent test programs. Repair was accomplished by cementing and riveting a hat section doubler over each damaged corrugation. Each doubler extended into and was attached to the vehicle's lower base ring, Figure 10. The two compensator mockups were removed. Rework of the converter tube structure was also carried out so that a firm and more positive method of tube-to-converter shell attachment technique could be evaluated. After repair and rework, the test unit was redesignated as the S10A-PSM-1R (reworked).

Since it was evident that several significant design changes were necessary for improving the structure (some already in progress), a continuation of the original test plan on the structurally damaged vehicle became relatively meaningless at this time. Consequently, several special tests were specified which would be useful in defining vehicle characteristics and response in localized areas of the unit. A continuation of this test effort is discussed in the following section.

The necessity of a completely reliable g-limiting device or an overload scram system to prevent the accidental over-loading of future systems was obvious from these first PSM-1 tests. Such instrumentation has since been procured and is in use on all present test programs requiring response control. This instrumentation incorporates both the g-limiting device and a scram system for double protection. Additionally, visual monitoring of meters recording important vehicle response points is still maintained.

E. SPECIAL TESTING PROGRAMS, PSM-1R

1. Resonant Frequency and Damping Rate Determination

Before any particular test programs could be started, it was important to determine by test, the resonances and response characteristics of the reworked test vehicle. Testing in the longitudinal direction established

3-28-62

Figure 10. Repair of Damaged Corrugations

7580-5156

the first fundamental resonant frequency at 74 cps. Prior to damage this resonance occurred at 80 cps.

Magnification factors at the new resonant frequency for two important vehicle locations are noted below. The values noted in the Z-Z direction are of the same order of magnitude as values noted in previous tests (Table 3)

Accelerometer Location	Orientation	Fundamental Magnification Factor
7 Upper converter load ring	Z-Z	10
7 Upper converter	Y-Y	3.5
126 Reactor base	X-X	6
126 Reactor base	Z-Z	14

To attain essentially rigid support at the base ring, the SNAP vehicle was bolted to the large slip table and low-level modal vibration surveys were conducted using Goodman Model V-47 shakers (2-lb force, rated output) attached to the upper converter load ring. The structure was found to have two, distinct, first fundamental lateral resonant frequencies resulting from a nonsymmetrical structure owing to converter shell repairs and/or NaK tube support modifications. One resonance occurred at 16 cps about an axis almost in line with the vehicle X-X axis; the other resonance occurred through an axis 90° removed from the other and at a frequency of 17.2 cps. In free vibration, the vehicle displayed only one resonance (16 cps), but superimposed on this vibration was a 1.2 cps beat caused by a coupling of the 16 and 17.2-cps resonant frequencies. Figure 11 shows the axes through which the two resonances occurred.

A first fundamental torsional mode, occurring at 60 cps, was found by applying a vibration force couple to the top converter ring approximately on the X axis (Figure 11). The torsional mode was measured by placing four accelerometers equally spaced around the top of the converter ring tangent to the X and Y axes and determining the frequency at which the accelerometers had responded in phase and at equal amplitudes. A survey of the converter shell was made during the torsional and bending tests to verify that the torsion

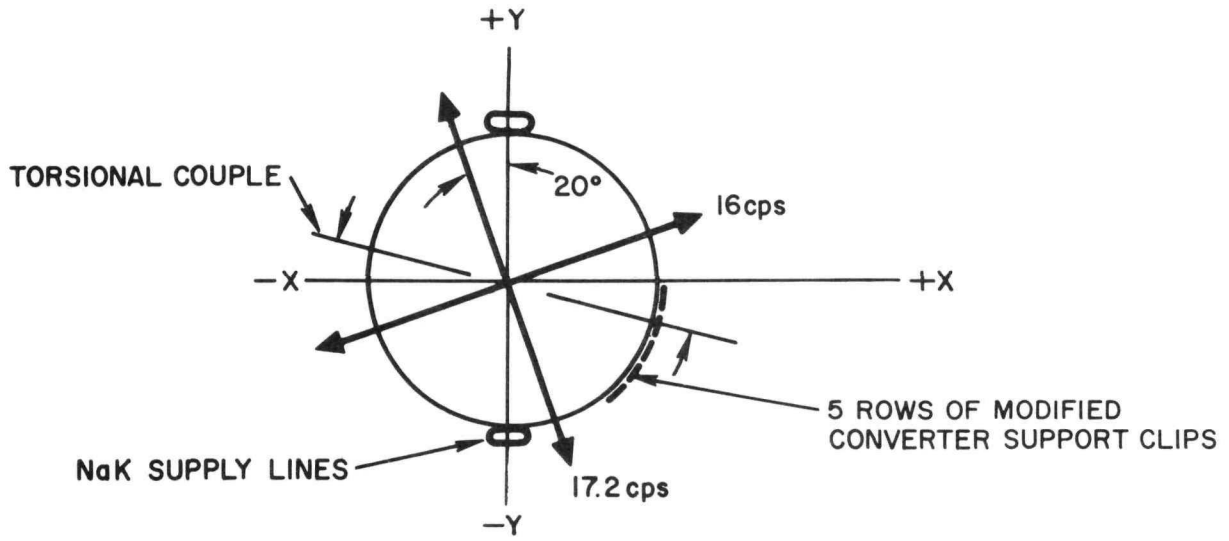

Figure 11. Location of Resonance Axes

and bending modes had been identified accurately. Plots of this data confirmed that the modes had been identified properly.

The decay curve of the unit was obtained by applying a manual impulse to the structure near the center of gravity and recording the decay rate of an accelerometer signal at the top of the converter. Calculations from the decay curve yielded 2% damping.

2. Low Level Tests, Longitudinal Axis (Z-Z)

The S10A-PSM-1R vehicle was subjected to longitudinal low-level vibration testing on the large Ling shaker system during the week of March 19, 1962. During testing, all vibration table inputs were maintained at less than 0.15 g. The response near the center of gravity was limited to 1.0 g at the top of the converter structure and 0.5 g at the reactor base box ring. The electronic g-limiting device (designed by the Environmental Laboratory Instrumentation Unit) controlled the system successfully throughout the vibration testing.

The converter support structure and NaK converter tubes were surveyed during constant octave sweep rates from low to high frequency, a 20 to 250-cps sweep requiring about 10 min. Sensors were located as shown in Figure 12. Maximum response of the modified skin-NaK tube assembly was 10 g's in the

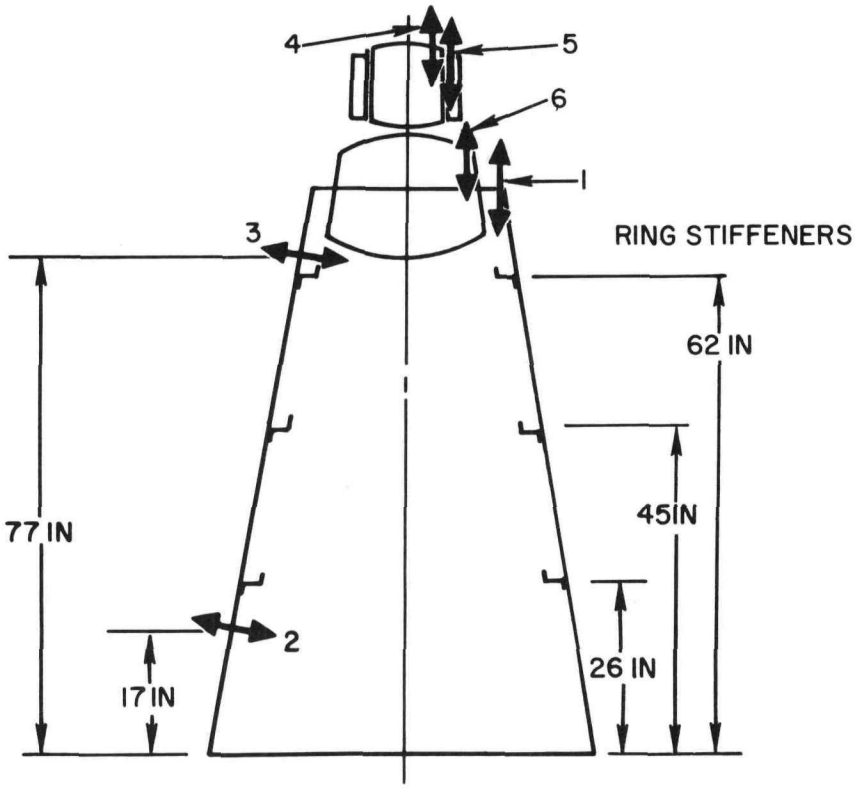

Figure 12. Accelerometer Locations S10A-PSM-1R
Low-Level Longitudinal Axis Surveys

radial direction with a 0.12 g longitudinal (Z-Z) table input. The area of greatest response occurred just above the repaired doublers on the convolutions between the +X and -Y axes. This was in the region of the most serious original damage and indicated that the shell's high-stress region shifted from the original damage point covered by the doublers to the skin area at the top end of the doublers. During these low level vibration sweeps, it appeared that a slight propagation of the cracks in the convolutions of the repaired converter shell was taking place. During subsequent testing, however, no change was noticed.

A survey of the reactor-shield structure indicated that the reactor structure resonated sharply at 150 cps with respect to the shield and converter structure. The resonance was transmitted back through the structure and showed up as a peak on most of the surveyed points, as shown in Table 20.

Further vibration testing of the PSM-1R was temporarily delayed so that an acoustic test might be conducted on the vehicle.

TABLE 20

ACCELEROMETER LOCATIONS S10A-PSM-1R LOW LEVEL LONGITUDINAL AXIS SURVEYS

Record No.	Item Position		Maximum Response for 0.12-g Input			
			72 cps		150 cps	
			g	Magnification	g	Magnification
	Converter	1	1.0	10	0.73	6.1
	Skin	2	9.5	79	2.4	20
	Skin	3	2.5	21	5	41
353	NaK tube	2	9.4	78	1.2	10
312	NaK tube	3	10.8	90	5.4	45
	Reactor cover	4	3.7	31	2.2	18.3
	Control	5	1.5	12.5	0.5	4.2
	Shield skin	6	1.0	8.3	0.36	3.0

3. Acoustic Tests

a. Transportation

In April 1962, the S10A-PSM-1R test unit was transported to the North American Aviation Acoustic Test Facility at Inglewood, California. No excessive shocks were observed during handling or transit.

b. Description of Test Facility

The North American Aviation Acoustic Test Facility (Figure 13) in Inglewood consists of a horn-shaped concrete building with a 3 by 5 ft throat leading into a catenary horn which expands into a reverberation chamber approximately 25 by 25 by 25 ft. The sonic drivers consist of a low-frequency siren, 50 to 2000 cps, and a high-frequency siren, 500 to 10,000 cps. Each siren is driven by a variable level direct current motor to provide frequency control. Sound pressure level is obtained by two 400 hp motor-driven air compressors supplying up to 2500 cfm to each siren. The output of the siren is sinusoidal, and the frequency is measured by tachometer generators mounted on the siren shafts. Sound pressure levels are measured indirectly by a microphone system located in the chamber and calibrated to correspond to previously determined decibel levels. A random output driver was not available at the time of this test. No remote viewing devices were provided

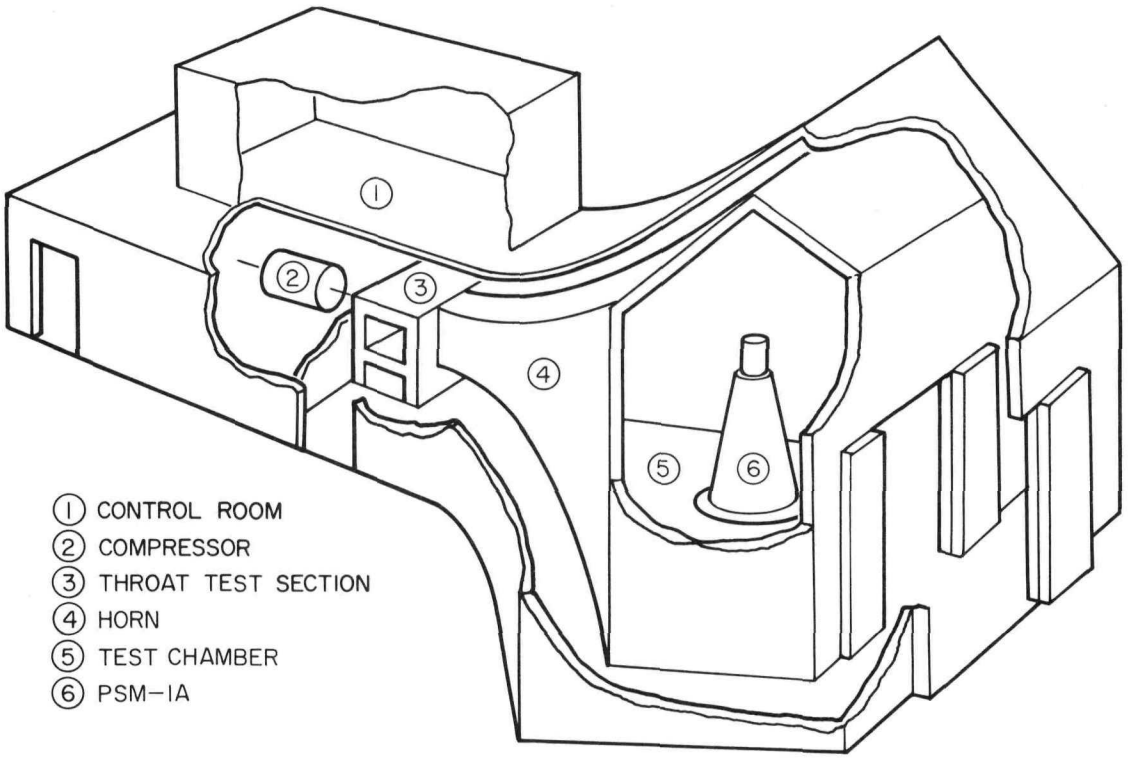

Figure 13. Acoustic Test Facility

in the structure in the interests of original construction economy. One channel of strobe light was available for visual monitoring when sound levels permitted personnel entry into the test room.

c. Test Procedure

Low-level acoustic sweeps were conducted on the vehicle which was installed in the test chamber as illustrated in Figure 13. Visual surveys were made by a strobe light, with the sound pressure level limited to 125 db as a safe operating maximum for personnel. The response at various points on the structure was surveyed at the first fundamental resonance of 56 cps. From this information, 9 accelerometer locations were selected by the SNAP 10A Engineering Unit personnel for final recording (Figure 14). Three accelerometers (1, 2, 3) were located on the internal skin of the nuclear power unit directly behind three other accelerometers (4, 5, 6) mounted on tubes at the stations noted. One accelerometer (7) was used to measure the skin adjacent to the tube area. The two remaining accelerometers (8, 9) were mounted on the upper converter load ring at the +X and -Y axes.

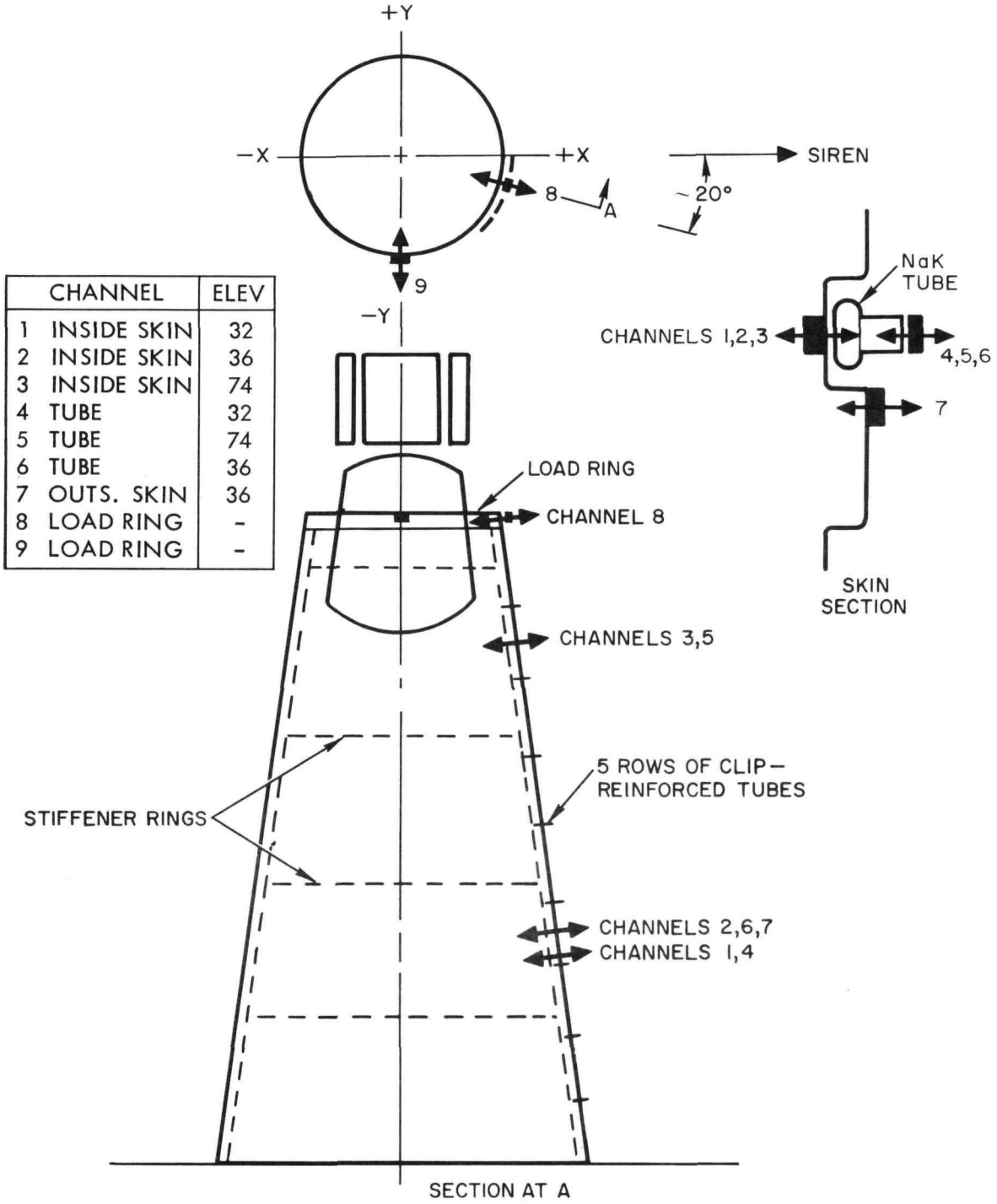

CHANNEL		ELEV
1	INSIDE SKIN	32
2	INSIDE SKIN	36
3	INSIDE SKIN	74
4	TUBE	32
5	TUBE	74
6	TUBE	36
7	OUTS. SKIN	36
8	LOAD RING	-
9	LOAD RING	-

4-15-64

7561-01262

Figure 14. Acoustic Test Accelerometer Locations

The acoustic sound pressure level test spectra (Figure 15) were furnished by the SNAP 10A Engineering Unit. A typical envelope of acoustic input is superimposed on one of the five specified test spectra on Figure 16.

Strain gage data were not recorded after it became apparent that no significant response was recorded on the strain gage channels at the SNAP Unit's longitudinal resonant point.

d. Results

The first fundamental response of the vehicle structure was observed at 56 cps, with a maximum response of 9 g on the converter shell skin at an elevation of 35 in. above the base. This response was observed under sound pressure levels of 125 db. Strobe light observation of 125 db at 56 cps revealed a bulging movement all around the skin structure, and, in particular, a twisting movement of individual NaK converter tubes and radiators about the axis of the tube. The shift of the first fundamental longitudinal resonance of the structure from 72 to 56 cps was due to the relatively soft mounting used on the sonic chamber floor.

Between 50 and 1000 cps, shell and NaK tube response indicated that the two structures moved together as a unit; i.e. in phase and at approximately the same amplitude. Above 1000 cps, the shell skin response was generally at a higher level than the tubes.

The response of nine monitor points on the structure is shown in Figures 17 through 22 over the frequency range of 50 to 7000 cps. A typical family of response curves for three sound pressure levels is plotted in Figure 19.

The frequency response points of NaK tubes and adjacent support structure were found at approximately the same frequencies noted in previous sinusoidal tests.

No damage to the structure was observed during testing. The cracked portions of the repaired structure were closely observed during testing, and no propagation of the cracks was noted.

Upon completion of the acoustic test program, the vehicle was returned to the Atomics International Environmental Test Laboratory for additional vibration testing.

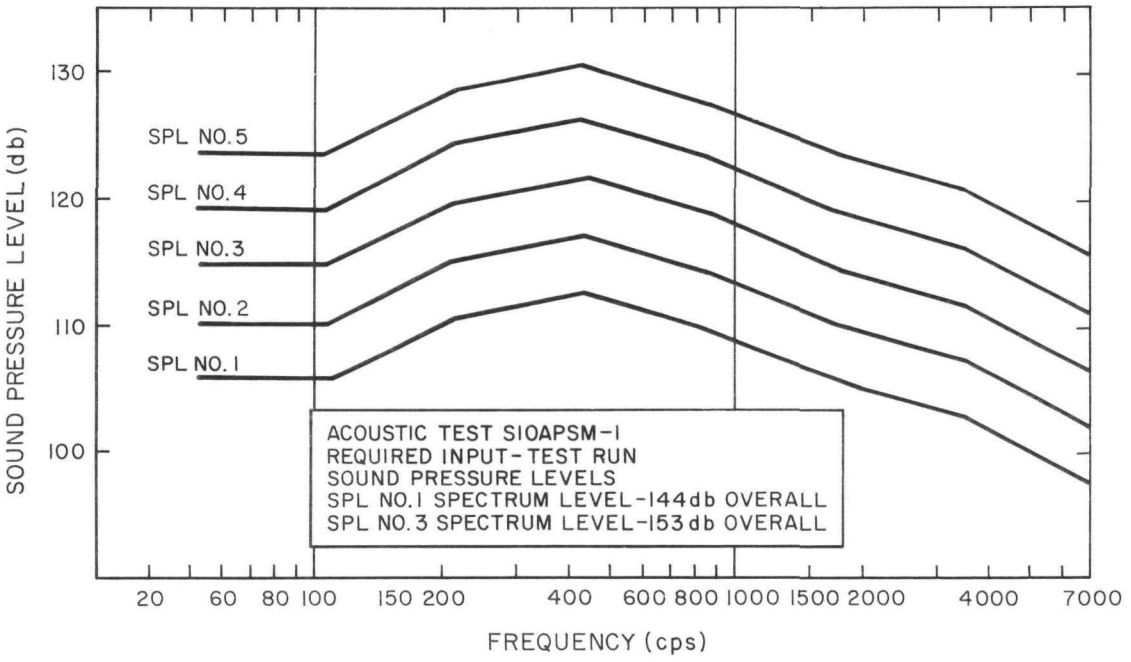

4-15-64 7561-01263

Figure 15. Required Acoustic Test Inputs

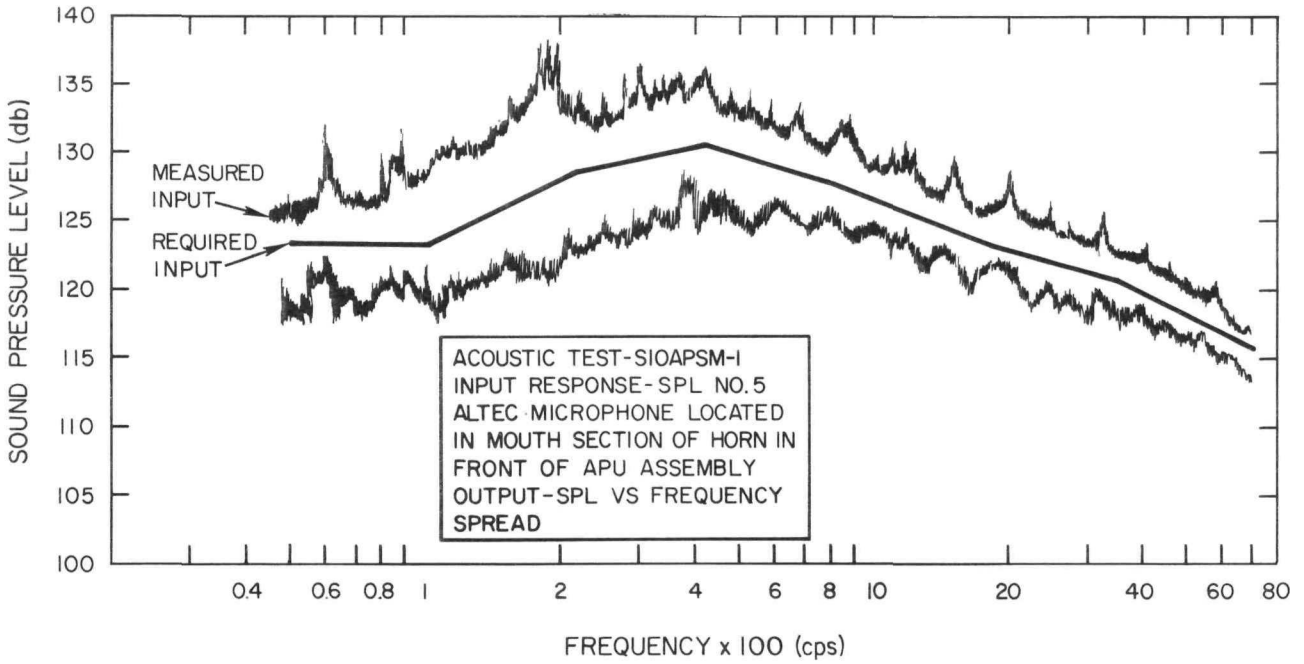

4-15-64 7561-01264

Figure 16. Typical Input Envelope

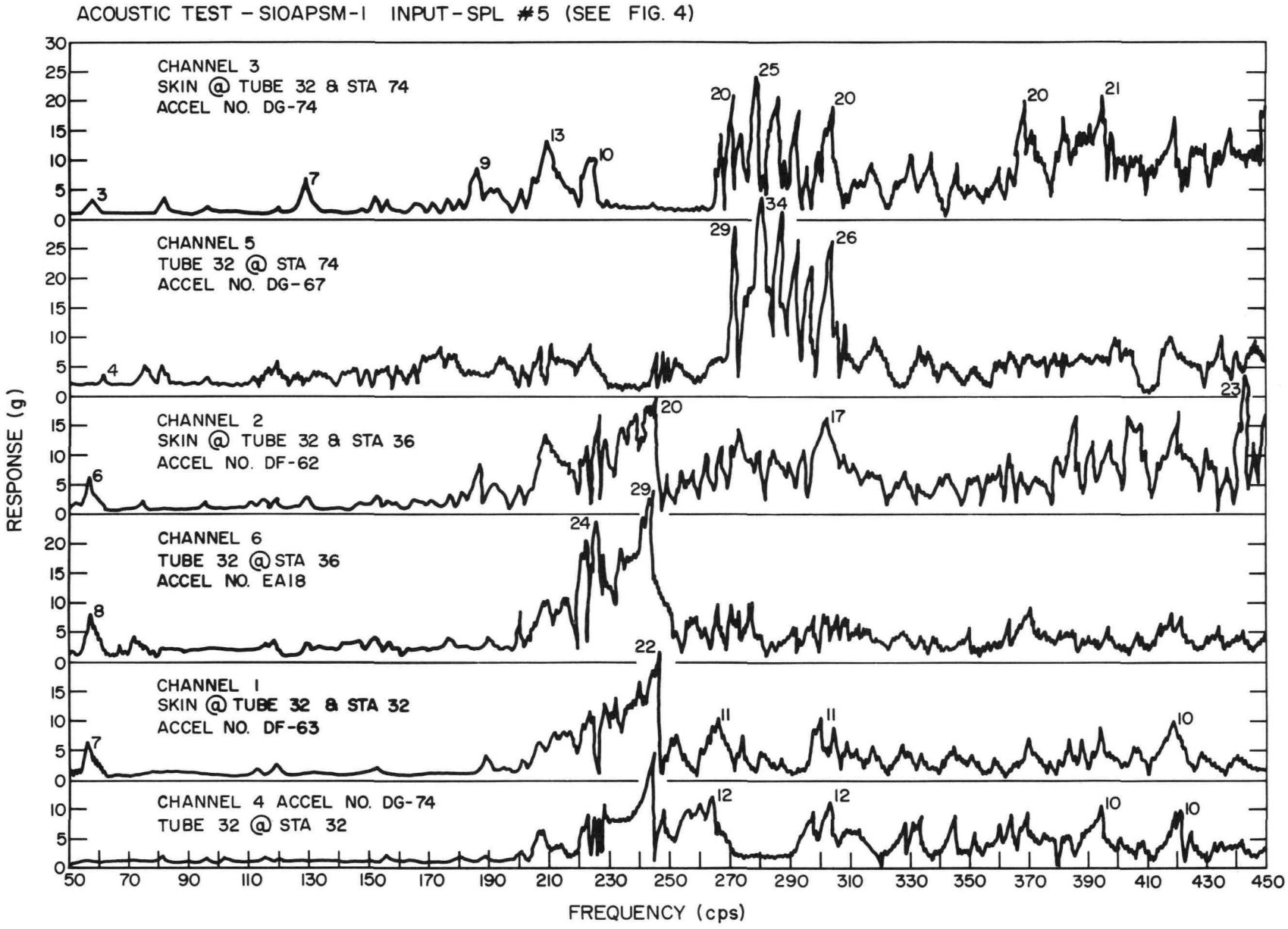

Figure 17. Vehicle Response to Applied Acoustic Inputs (1 of 2)

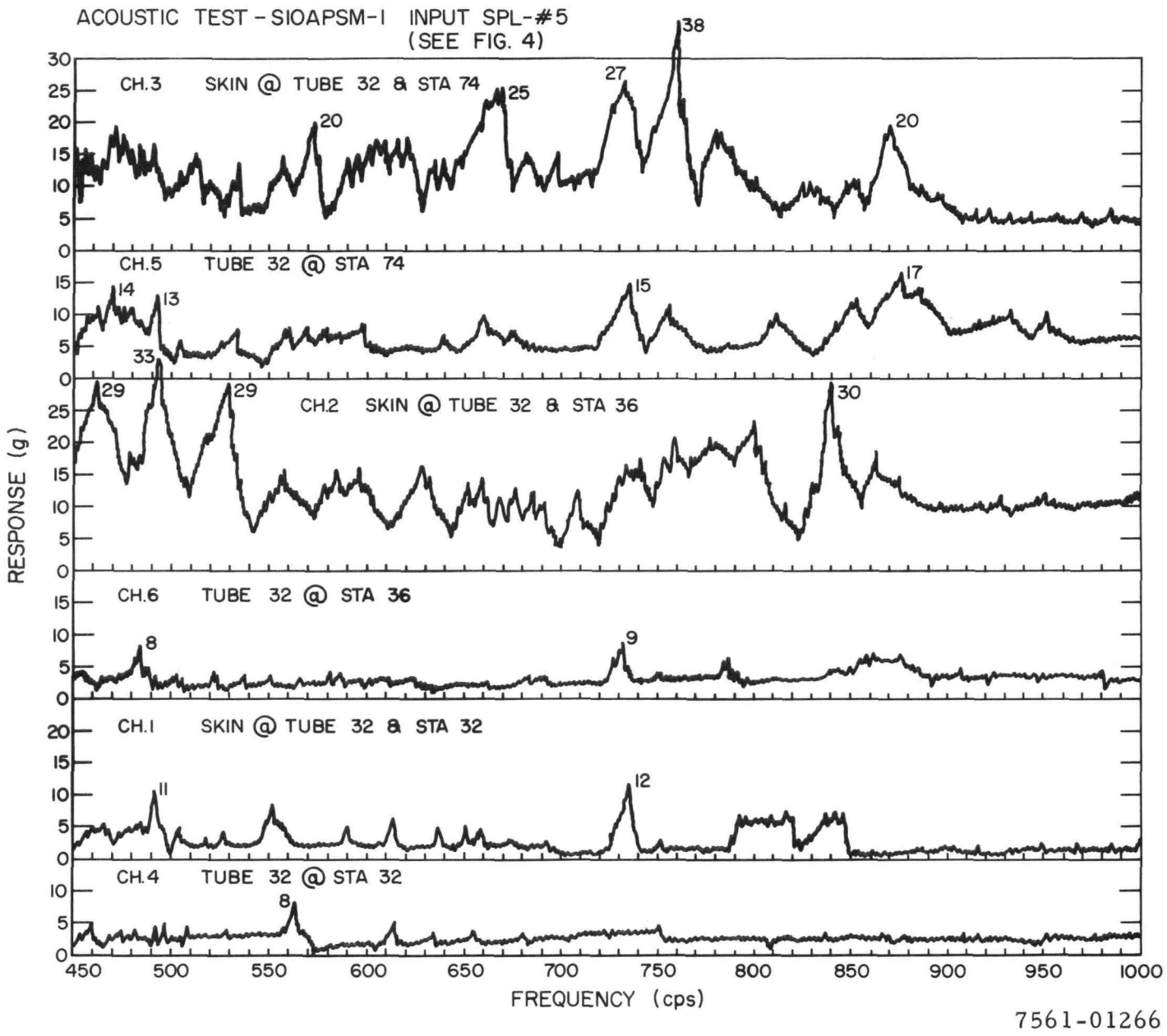

Figure 18. Vehicle Response to Applied Acoustic Inputs (2 of 2)

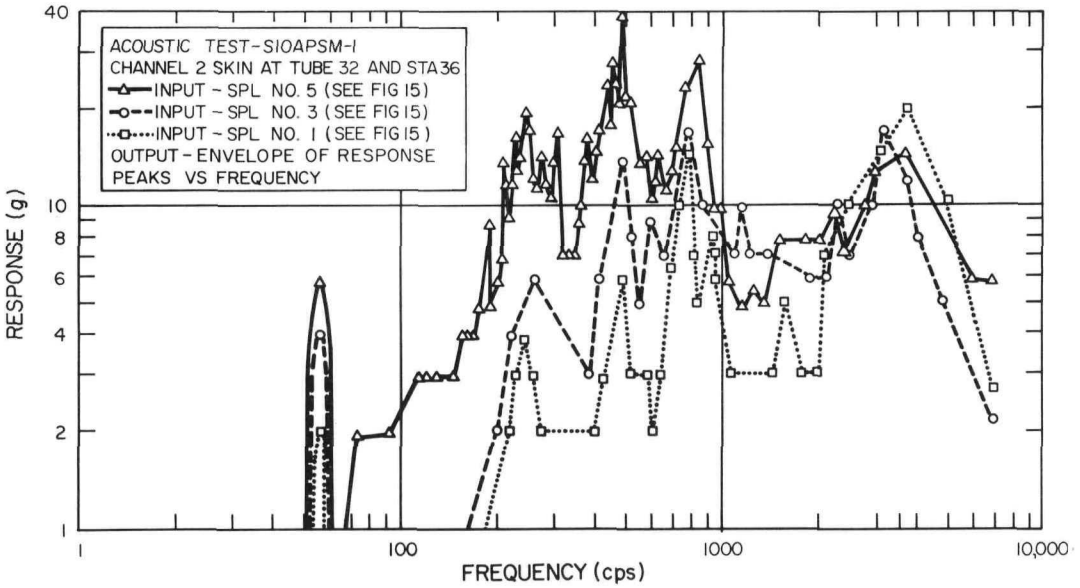

4-5-64 7561-01267

Figure 19. Typical Family of Response Curves for Three Sound Pressure Levels

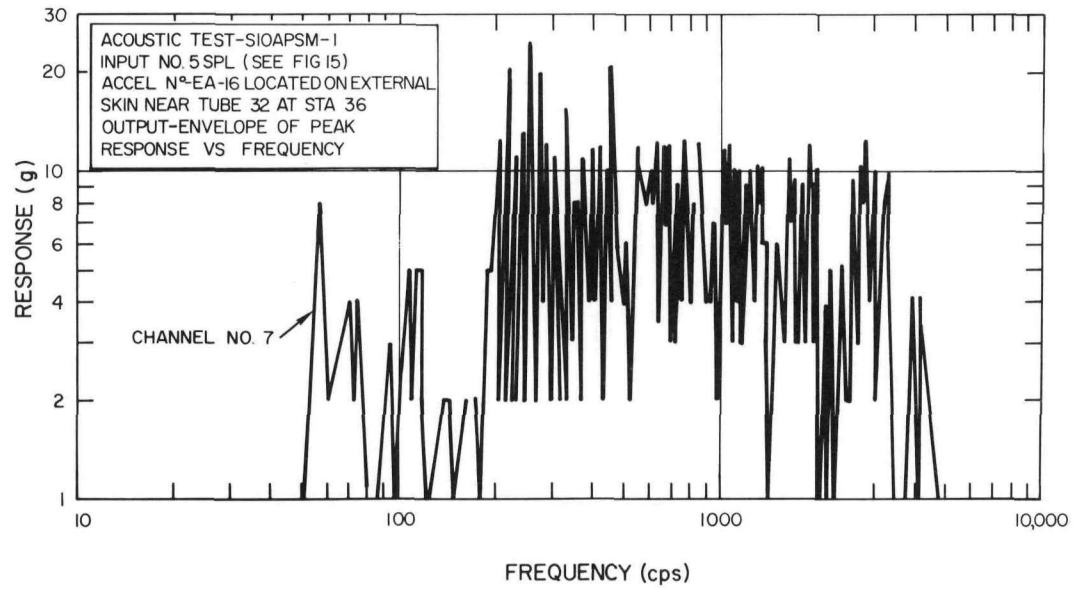

4-15-64 7561-01268

Figure 20. Vehicle Response to Applied Acoustic Inputs (1 of 3)

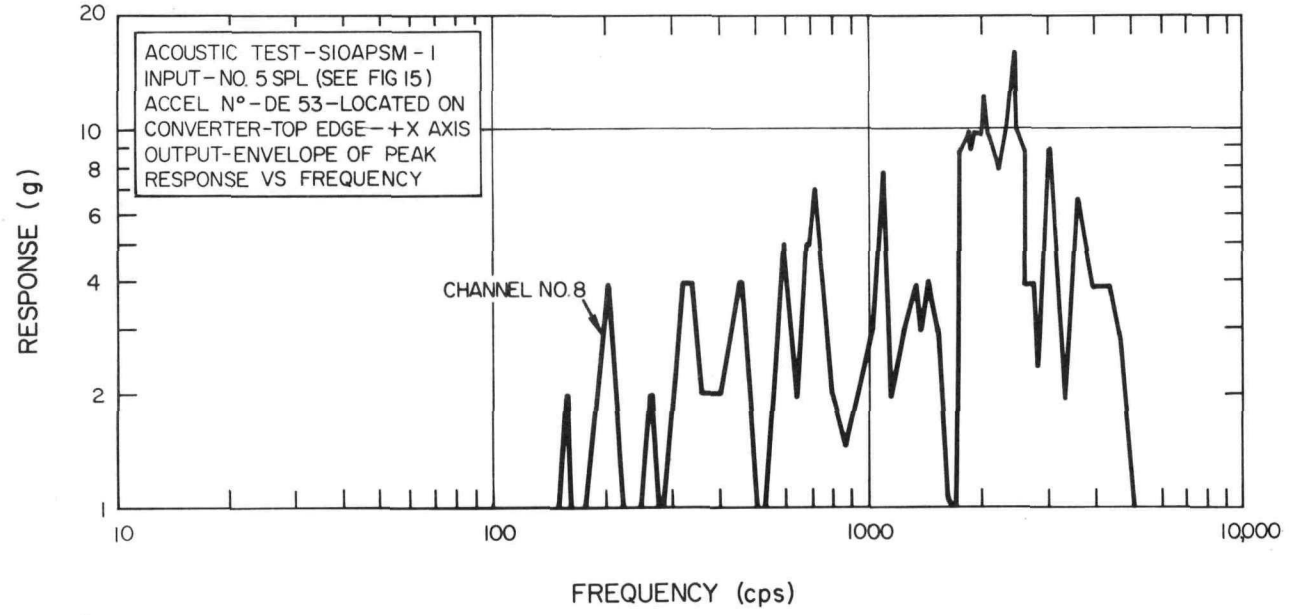

4-15-64 7561-01269

Figure 21. Vehicle Response to Applied Acoustic Inputs (2 of 3)

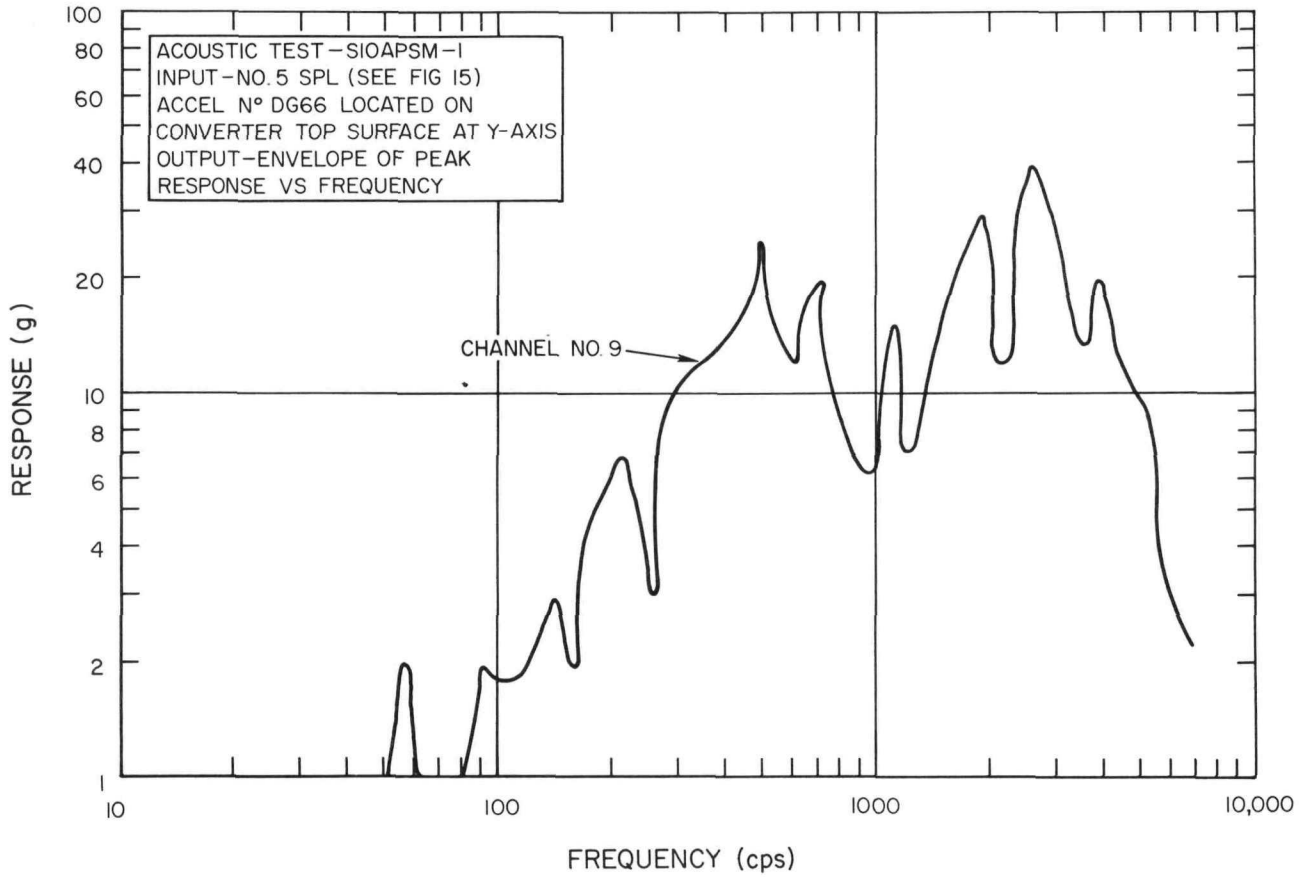

4-15-64 7561-01270

Figure 22. Vehicle Response to Applied Acoustic Inputs (3 of 3)

4. Lateral 100% Vibration Tests, 200 to 3000 cps

The S10A-PSM-1R vehicle underwent a lateral vibration test at 100% of the specified inputs for the purpose of comparing the skin and NaK converter tube responses with those noted in the acoustic test. The vehicle was rigidly bolted to the 30,000-lb shaker-slip table; the acceleration input was controlled by accelerometers mounted on the vehicle base ring. A five channel g limiting servo system restricted the output response of the SNAP unit's center of gravity. Accelerometers mounted on the vehicle skin and NaK converter tubes included the same positions as those used in the acoustic testing (Figure 23).

The accelerometer response vs frequency is plotted in Figure 24, 25, and 26. The maximum responses of the NaK tube and skin excited by the vibration test were approximately one-half the magnitude of the responses noted in the acoustic test (10 to 15 g vs 20 to 30 g).

5. Lateral 100% Vibration Tests, 27 to 200 cps

A test run was requested by the SNAP 10A Project in which the vehicle would be subjected to 100% lateral vibration levels over the 27 to 200 cps of frequency band. The purpose was to ascertain vehicle and component response at 100% levels with the shield structure revised to simulate a design change which occurred at that time. The change consisted of removing the four top brackets which tied the reactor support legs and the shield together. Shield support was now limited to the shield support flange and associated converter shell support brackets.

With the vehicle bolted rigidly to the 30,000-lb slip table at the base ring, an input of 1.7 g was applied at a constant octave sweep rate progressing from 20 to 200 cps in about 10 min. The electronic limiter controlled the response at the vehicle's center of gravity to 2.0 g. Vibration tests were conducted on the X axis, Y axis, and diagonally on the X-Y axis as shown in Figure 23. Instrumentation locations were the same as seen in Figure 23.

A typical abstract of three major resonance points is shown in Table 21. The first major resonance point which occurred was the tube bundle and skin resonance at 38 cps. This was in close agreement with the 42 cps observed in initial tests on the PSM-1 structure (Table 10). Since the testing was started at 27 cps, the first bending frequency of about 16 cps was avoided.

ACCEL NO.	DIRECTION	LOCATION
1	X	PUMP
2	Y	PUMP
3	X	REACTOR TOP
4	Y	REACTOR TOP
5	X	REACTOR BASE
6	Y	REACTOR BASE
7	X	SHIELD TOP
8	Y	SHIELD TOP
9	X	CONV. RING
10	X-45°	CONV. RING
11	Y	CONV. RING
12	X	SHIELD RING
13	Y	SHIELD RING
14	RADIAL,	TUBE 32 ELEV 74"
15	RADIAL,	TUBE 32 ELEV 72"
16	RADIAL,	TUBE 32 ELEV 36"
17	RADIAL,	TUBE 32 ELEV 32"
18		TABLE

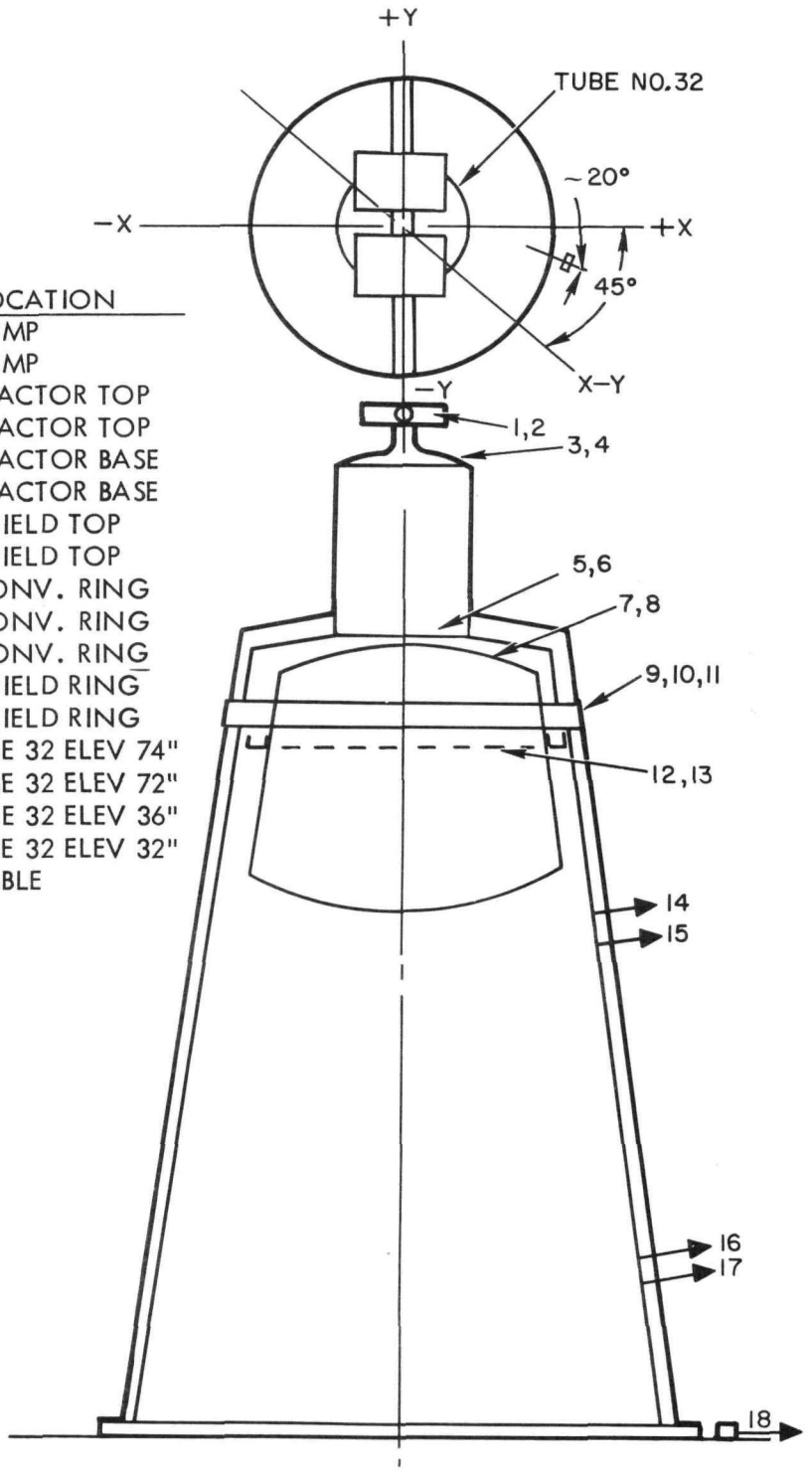

4-15-64

7561-01271

Figure 23. Accelerometer Locations – S10A-PSM-1R 200 to 3000 cps Lateral Vibration Test

The second resonance point at 56 cps compares with the acoustic test, which also excited the skin structure at 56 cps.

The 97-cps mode listed in Table 21 is the point at which the reactor-shield structure resonated with respect to the skin and tube structure. This resonant point was noted at 150 cps on the previous low level testing. The reduced resonant frequency stems from deletion of the four shield-to-reactor leg support brackets.

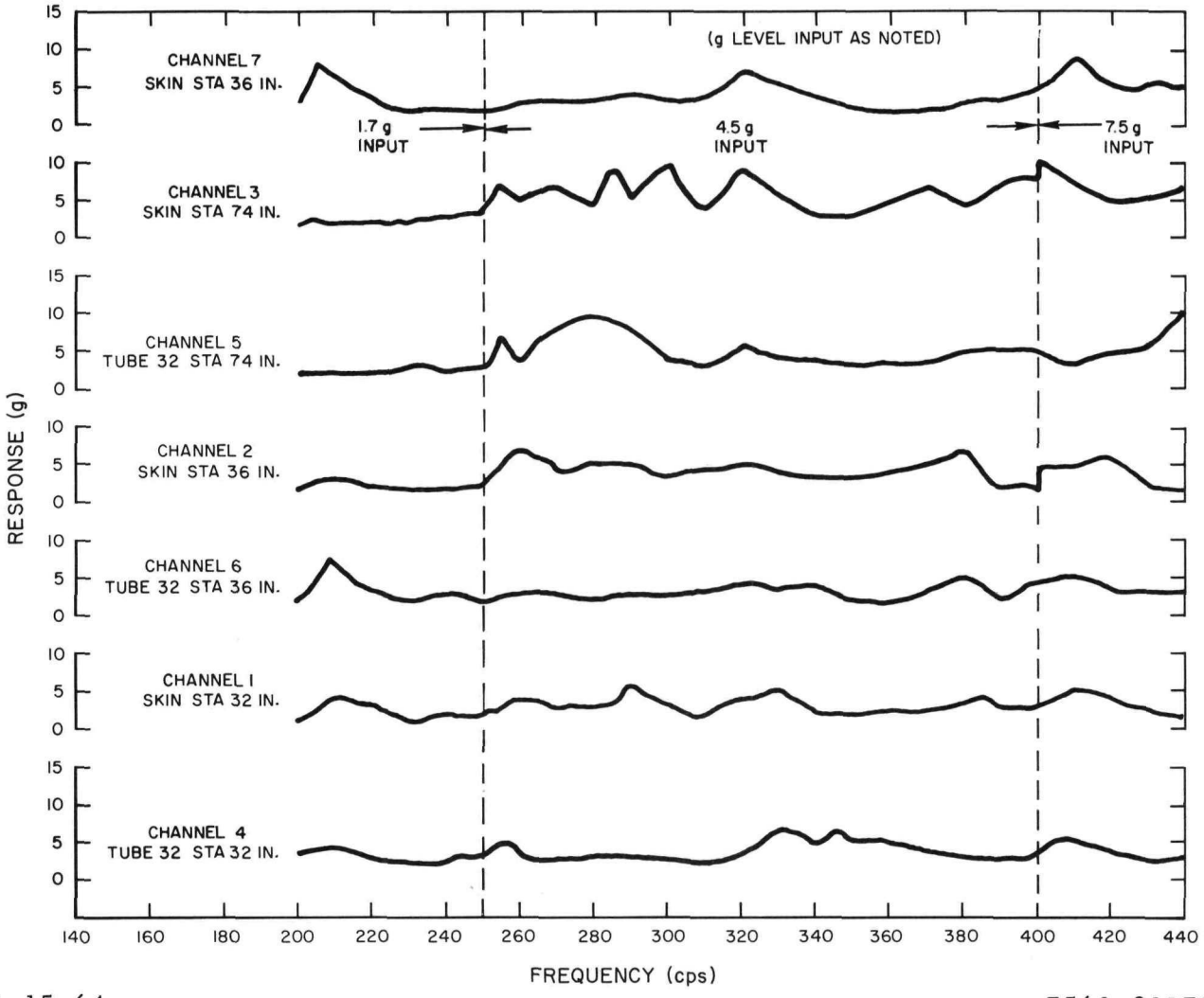

4-15-64 7561-01272

Figure 24. S10A-PSM-1R 100% Vibration Test, Lateral Axis
(1 of 3)

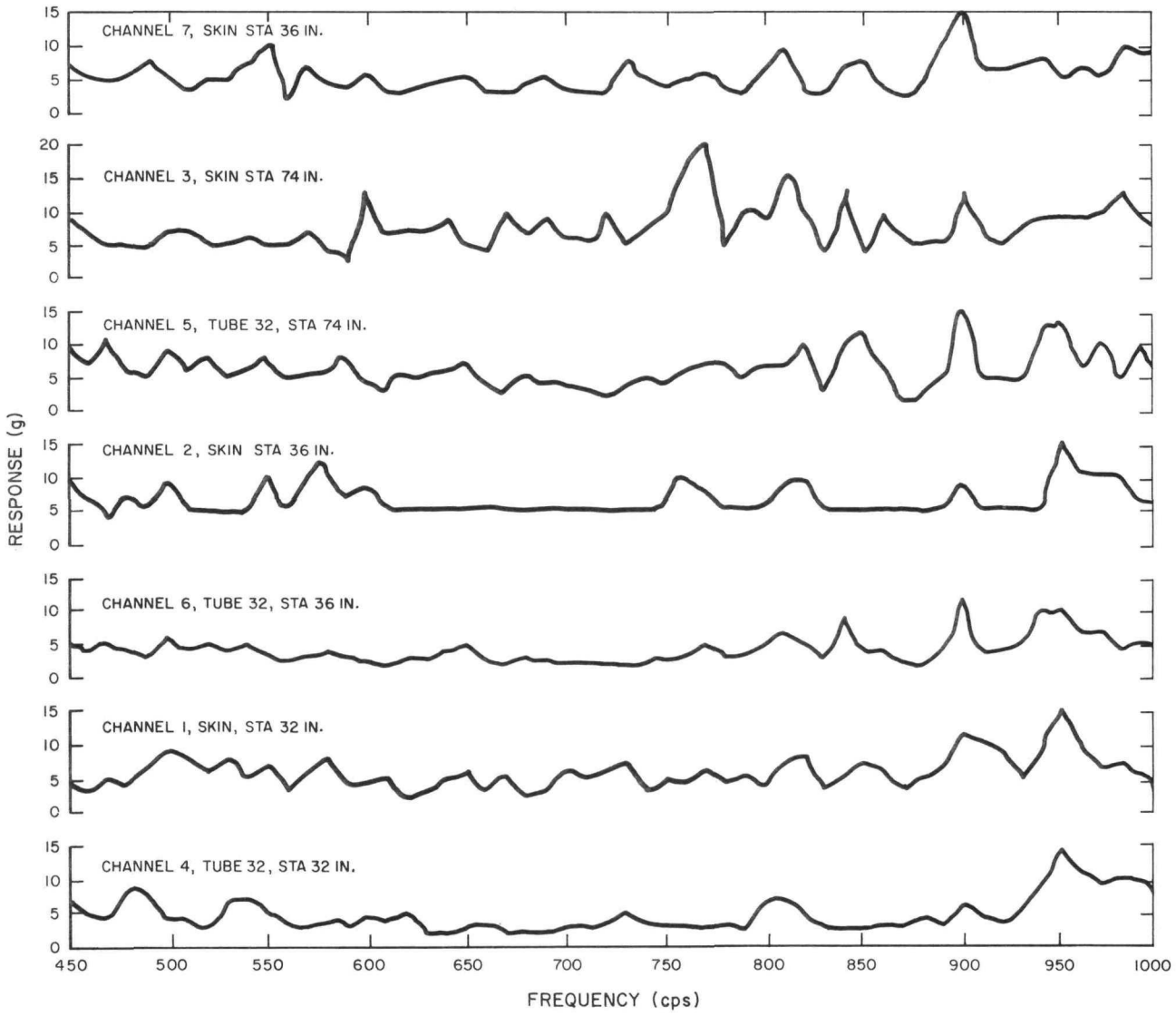

4-15-64 7561-01273

Figure 25. S10A-PSM-1R 100% Vibration Test, Lateral Axis (7.5 g) Input (2 of 3)

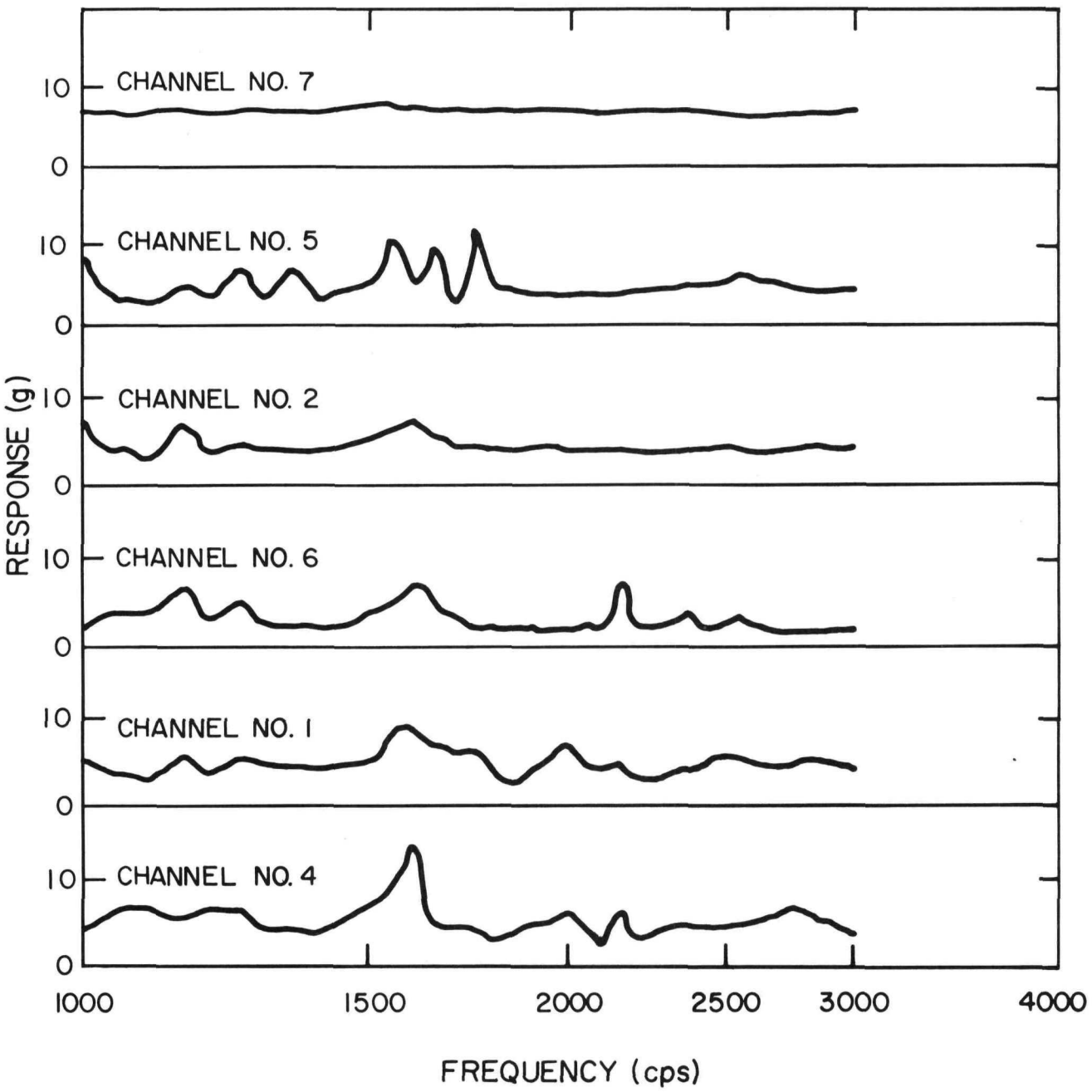

4-15-64 7561-01274

Figure 26. S10A-PSM-1R 100% Vibration Test, Lateral Axis (7.5 g) Input (3 of 3)

TABLE 21

S10A-PSM-1R 100% LATERAL VIBRATION TESTS 27 to 200 cps ACCELEROMETER RESPONSE, g (1.7 g input)

Channel	Shake Axis	Accelerometer Direction	Frequency (cps)		
			38	56	97
	X-X	X-X	7.8	2.2	3.4
1	Y-Y	X-X	1.3	0.88	0.50
	X-Y	X-Y	4.2	1.3	2.9
	X-X	Y-Y	1.6	0.45	1.36
2	Y-Y	Y-Y	2.9	0.55	1.7
	X-Y	Y-Y	2.5	0.96	0.8
	X-X	X-X	9.8	0.7	0.7
3	Y-Y	X-X	6.0	0.50	0.30
	X-Y	X-Y	9.0	5.0	0.36
	X-X	Y-Y	3.5	0.44	2.3
4	Y-Y	Y-Y	3.6	0.45	0.75
	X-Y	Y-Y	3.7	0.10	0.72
	X-X	X-X	8.7	0.7	2.3
5	Y-Y	X-X	0.72	0.35	0.28
	X-Y	X-Y	2.5	0.10	0.52
	X-X	Y-Y	5.0	0.56	2.3
6	Y-Y	Y-Y	2.0	0.70	1.4
	X-Y	Y-Y	2.5	0.10	0.72
	X-X	X-X	6.2	1.7	4.2
7	Y-Y	X-X	1.2	0.85	0.35
	X-Y	X-Y	4.0	1.1	2.8
	X-X	Y-Y	2.9	0.80	1.0
8	Y-Y	Y-Y	2.9	1.0	1.3
	X-Y	Y-Y	2.4	1.0	1.0
	X-X	X-X	17.5	3.2	4.0
9	Y-Y	X-X	1.25	2.6	1.1
	X-Y	X-X	3.5	1.0	2.1
	X-X	X-Y	0.10	0.10	0.10
10	Y-Y	X-Y	1.7	1.5	0.78
	X-Y	X-Y	0.10	0.10	0.10
	X-X	Y-Y	8.0	2.7	2.0
11	Y-Y	Y-Y	2.9	1.5	1.1
	X-Y	Y-Y	4.2	0.95	0.85
	X-X	X-X	13.5	3.7	5.1
12	Y-Y	X-X	3.6	1.5	0.66
	X-Y	X-Y	4.0	7.5	3.0
	X-X	Y-Y	2.0	0.82	1.5
13	Y-Y	Y-Y	2.4	0.65	1.2
	X-Y	Y-Y	2.4	0.55	0.75
	X-X	Radial	20.0	10.8	5.2
14	Y-Y	Tube	2.2	7.5	5.1
	X-Y	32	12.0	5.0	4.2
	X-X	Radial	16.0	7.8	5.0
15	Y-Y	Tube	2.1	5.2	3.1
	X-Y	32	14.0	5.6	3.5
	X-X	Radial	16.5	12.0	6.2
16	Y-Y	Tube	1.2	3.5	2.5
	X-Y	32	7.0	4.0	5.0
	X-X	Radial	14.0	11.0	5.0
17	Y-Y	Tube	1.5	4.0	2.5
	X-Y	32	9.0	3.0	3.5
	X-X	X-X	2.4	2.2	2.1
18	Y-Y	Y-Y	1.1	1.5	1.6
	X-Y	X-Y	1.0	1.7	1.5

BLANK

III. HIGHWAY TRANSPORTATION VIBRATION AND SHOCK TEST

A. INTRODUCTION

The shock and vibration loads sustained by a SNAP system during highway transportation must be controlled to prevent damage. The intensity of the shock and vibration inputs caused by road surface irregularities is normally attenuated, but sometimes amplified, by the vehicle's spring system and shock isolation mounts. These inputs are so varied that the road test is the most feasible way of obtaining useful data.

The transportation system of a shock-mounted* mass mockup of the SNAP 10A system to Edwards Air Force Base for a sled test acceleration program afforded a road test using a noncritical vehicle simulating the mass distribution and dynamic responses of subsequent sensitive S10A systems. The mass mockup was mounted in the rocket sled to be used for the acceleration tests and transported to Edwards Air Force Base on an air-ride, low-bed trailer pulled by an air-ride tractor (Figure 27). Shock and vibration data from both truck and mass mockup were recorded by two Impactograph recorders and a nine-channel electronic shock and vibration recorder.

Emphasis was placed on obtaining data relating both the response of the truck to the road inputs and the response of the mockup's mass center to inputs from the truck. During the trip, the rocket sled was fastened securely to the truck bed. The stiffness of the sled resulted in the response of the truck to the road inputs becoming the input to the mass mockup. All possible road conditions and truck maneuvers were investigated and all efforts to impart excessive shock or vibration loads to the center of mass failed.

---

*The Environmental Test Unit designed a shock mount system that would isolate the test specimen from rail induced vibration during the sled test program. Eight Lord shock mounts (two at each corner of the specimen cradle) were used; the resonant frequency of the suspension (12 to 13 cps) was made to fall under the fundamental resonant frequency of the test vehicle (17 to 18 cps). For highway transportation, two automobile shock absorbers were utilized on the forward end of the suspension to prevent excessive vertical displacement at the resonant frequency of the system since the 12 to 13 cps resonant range coincided with the frequency of probable truck inputs.

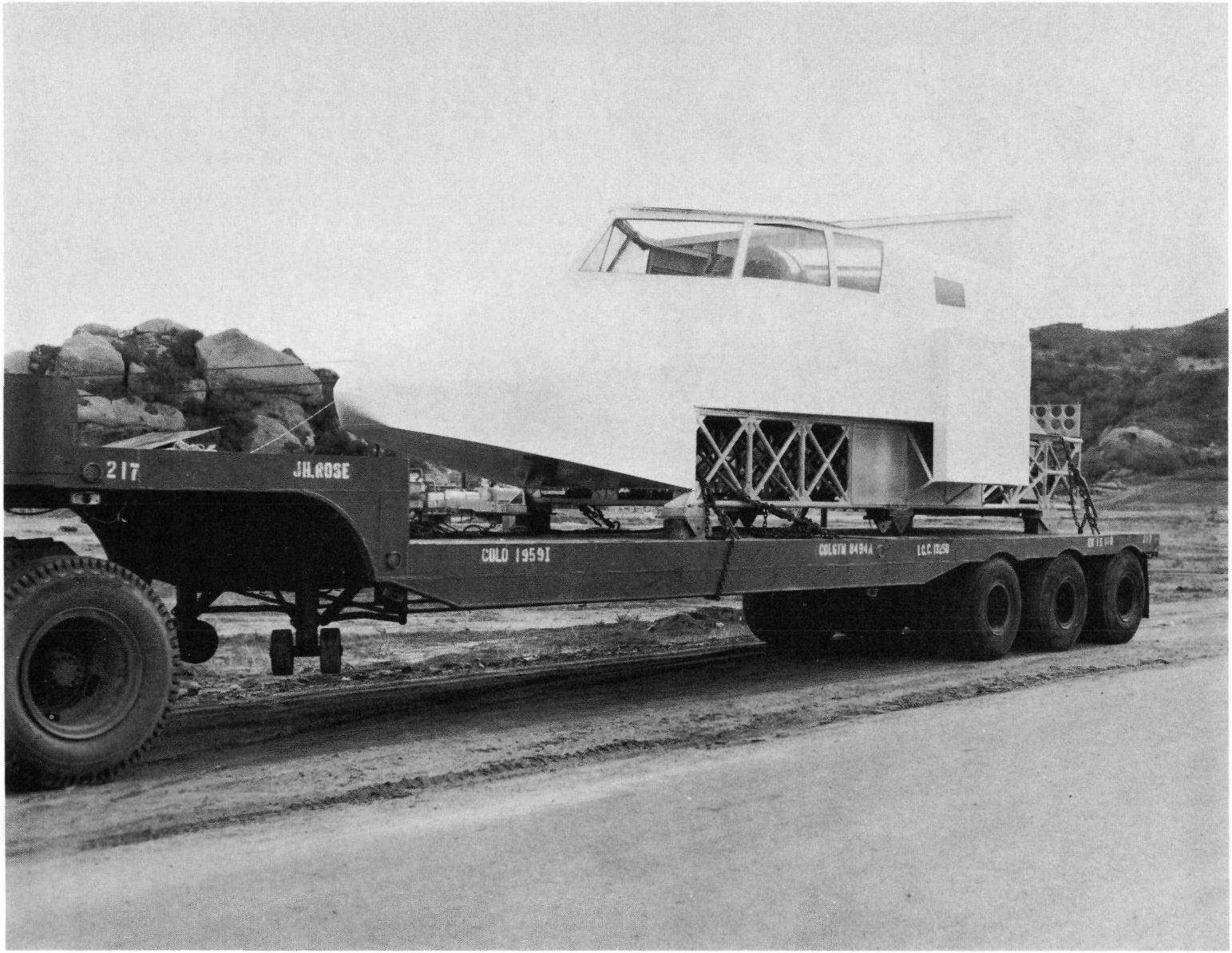

12-15-61

7580-1899B

Figure 27. Sled Mounting on Low Bed Truck

B. INSTRUMENTATION

At Atomics International, the portable instrumentation was limited to Impactographs which had not been evaluated under actual road conditions. To obtain reliable data, the testing service of Microdot Inc. was retained.

Placement of the Impactographs and the nine accelerometer pickups is shown schematically in Figure 28. Three accelerometers measured the axial responses midway between the rear mounting pads of the mass mockup cradle. One Impactograph and three accelerometers measured the response of truck and sled along three axes under the mass mockup center of gravity. The second Impactograph and three accelerometers were mounted as near as possible to the mass mockup's center of mass to measure its response along the three axes.

C. PRELIMINARY ROAD TESTS

On December 15, 1961, the mass mockup and rocket sled were ready for shipment to Edwards Air Force Base. After the road test instrumentation was installed and calibrated, the truck was driven over the asphalt roads at Santa Susana to check instrument sensitivities. The riding characteristics of the mass mockup were monitored visually. Microdot's standard test was used. This consisted of driving at a constant 15 mph over five 2 by 6 in. by 10 ft boards placed across the road and spaced 25 ft apart.

Accelerometer and Impactograph records showed that the instruments were operating at the right sensitivity. No detailed data reduction was made as changes in the mass mockup support system had to be made. A second successful preliminary road test was made prior to the trip to Edwards Air Force Base.

D. ROAD TEST TO EDWARDS AIR FORCE BASE

In this test it was desired to simulate as nearly as possible the various road and/or driving conditions which could be encountered in a typical truck transport of a critical test package. Consequently, every effort was made during this trip to impart excessive shock loads to the dummy unit. Rough road was purposely encountered at both slow and fast speeds, rail crossings were crossed at higher than average speeds, highway runs were made with the right wheels riding on the shoulders, and quick starts and stops were conducted. The truck speed, odometer readings, and road condition were recorded at each point of interest. Sixty-seven records were made in this manner.

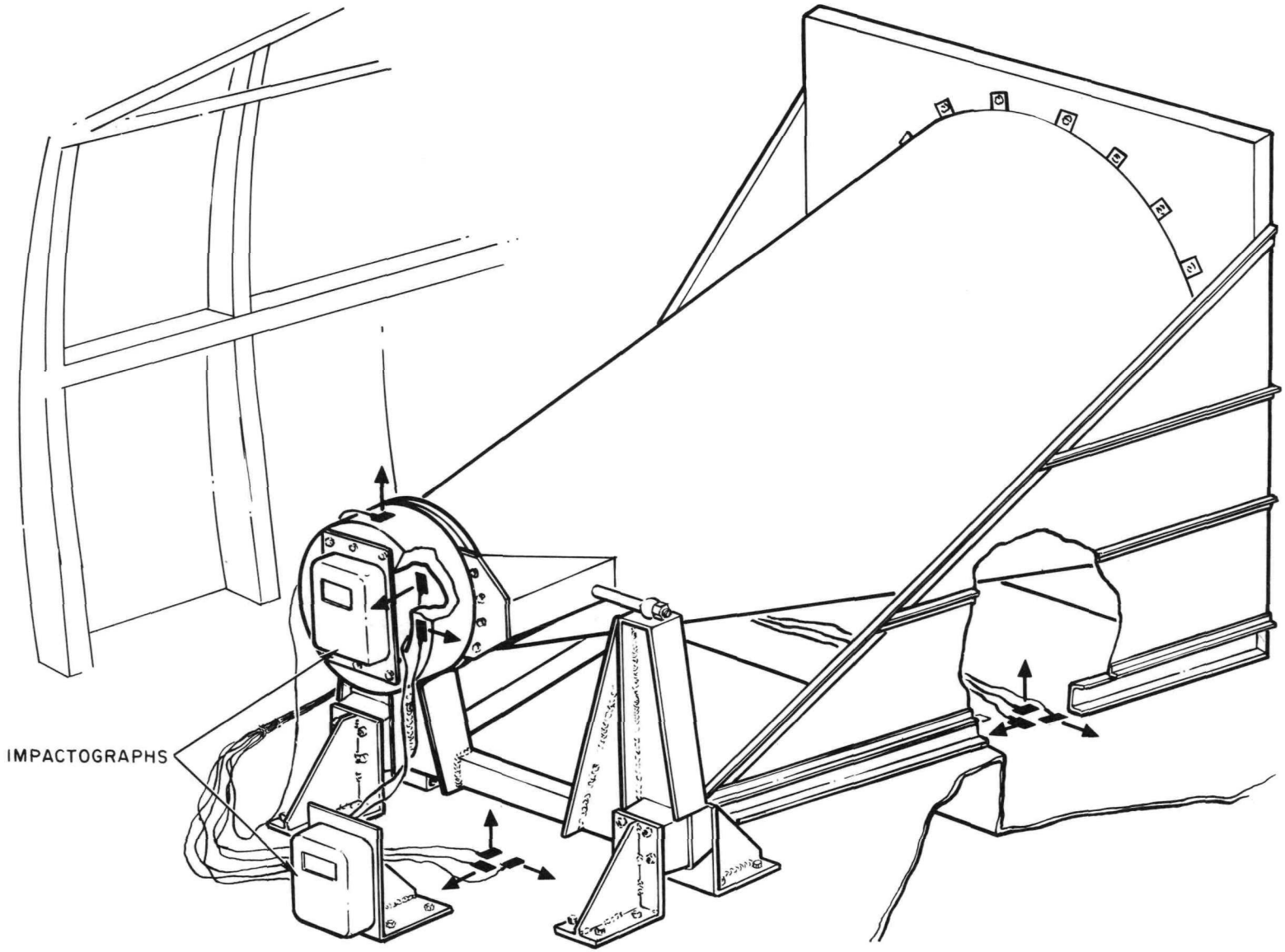

Figure 28. Accelerometer Locations on Sled and SNAP 10A Mass Mockup

After the 3-hr and 45-min trip over the route shown in Figure 29, the oscillograms were brought back to Santa Susana for processing and data reduction. Only eleven records merited interest, two of them showing accelerations which exceeded 2 g.

Responses in excess of 2 g occurred twice on Devonshire at 35 mph. Record 726 (Figure 30) was taken as the truck passed over a bump near Winnetka Avenue. It was immediately apparent that the mass mockup was undergoing greater accelerations than the sled. The mass mockup would have ridden more gently if secured to the sled. Its fore and aft accelerations, also greater than those of the sled, had to be the result of cross coupling from the vertical input. Such cross coupling occurs when the center of elastic suspension does not coincide with the center of gravity of the supported system. This was the case with the mass mockup-cradle suspension system. (The axial nomenclature relates to the transport system and not to the launch axes of the SNAP system.)

Road surface irregularities often occur when changing from one type of surfacing to another. The second record (oscillogram 727, Figure 31) showed accelerations in excess of 2 g on Devonshire Street at Zelzah Avenue, where there was a change from concrete to asphalt. The +2.34 g vertical acceleration was the maximum response recorded during the test run, and the 1.7 g forward acceleration was the largest longitudinal response. The truck kept below 10 mph on very rough sections of road. Some deliberate high-speed tests were made, such as on the crossing of two overpass bridges on Highway 6.

The Impactograph records showed the greatest deflection when the electronic recording systems showed the greatest inputs. The relative response of the two systems, however, was not constant. Lack of correlation between the two systems led to an investigation of the Impactograph's frequency response. As the frequency of a constant acceleration vibration input varied from 5 to 16 cps, the response of the Impactograph changed by a factor of three; the maximum response occurring at 13 cps. Since the truck inputs to the sled generally fell in the 5 to 16-cps range, no quantitative reduction of the Impactograph data was attempted.

This test showed that it was feasible to transport SNAP systems over the highways without exceeding specified maximum allowable shock or vibration values. The use of air-spring trucks of proper load capacity and proper packaging, alert careful driving, and foreknowledge of the road conditions are sufficient to limit the response of the transported package to less than 2 g.

BLANK

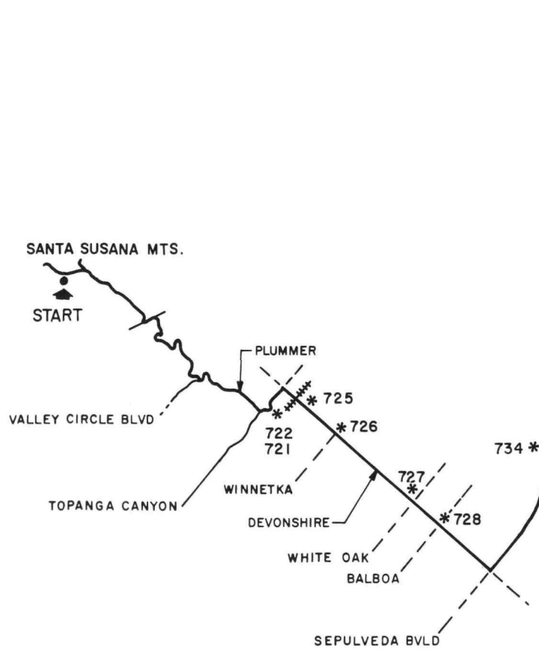

SAN FERNANDO VALLEY

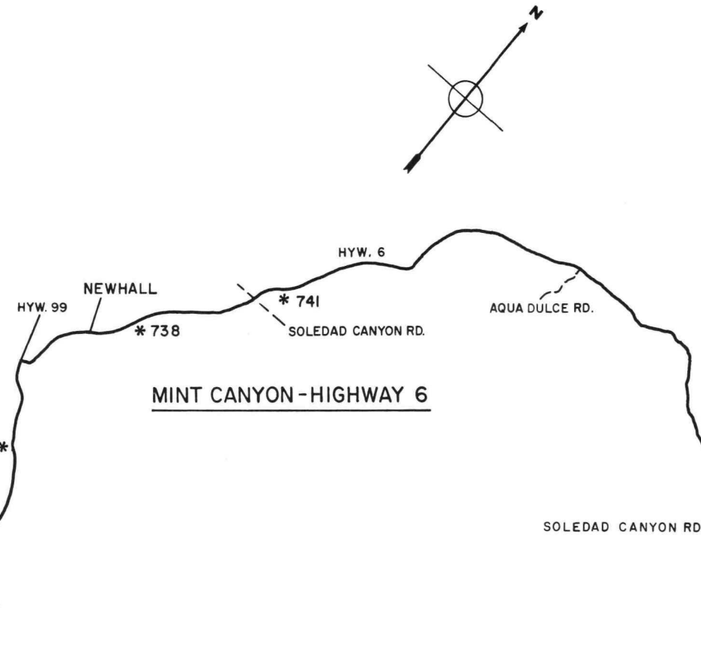

MINT CANYON - HIGHWAY 6

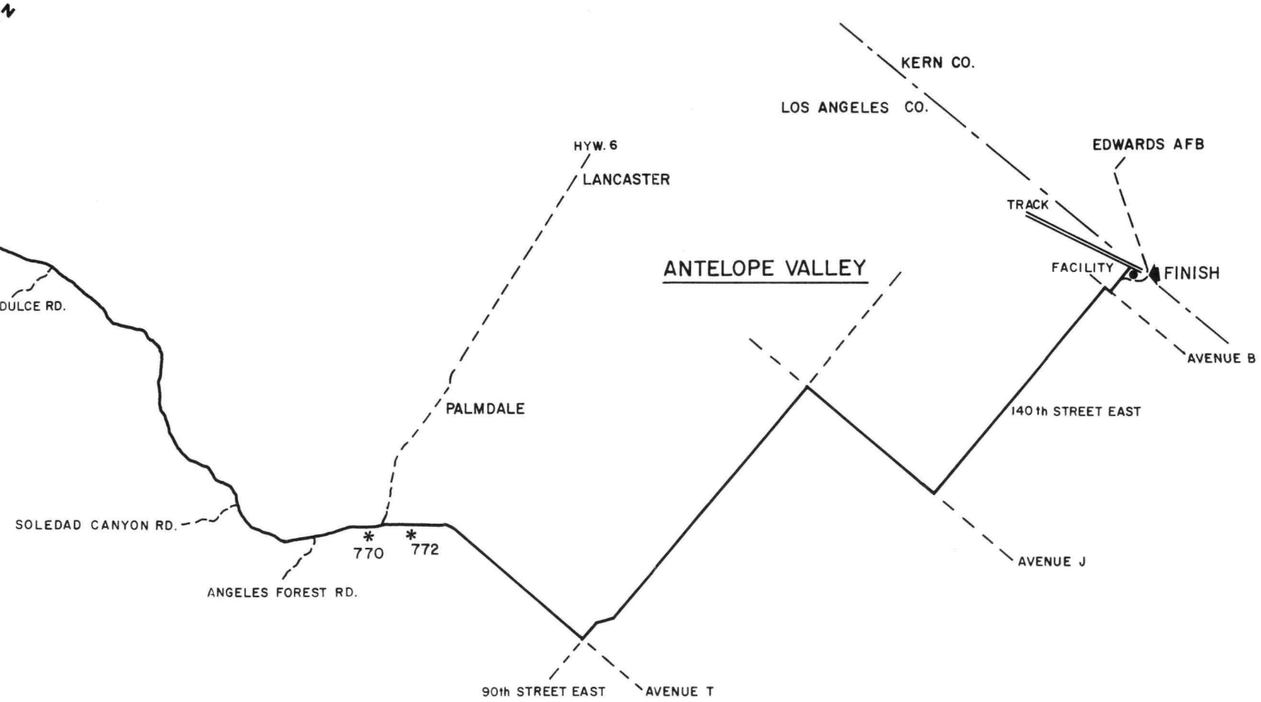

4-1-64 7561-01276

Figure 29. Highway Transportation Route

BLANK

Oscillogram No. 726
Location: Devonshire St. near Winnetka Ave.
Road Condition: Bump on Road
Maximum Acceleration: Vertical Positive 2.25 g Negative 0.20 g
Lateral Right 0.26 g Left 0.20 g
Longitudinal Fore 1.18 g Aft 0.65 g

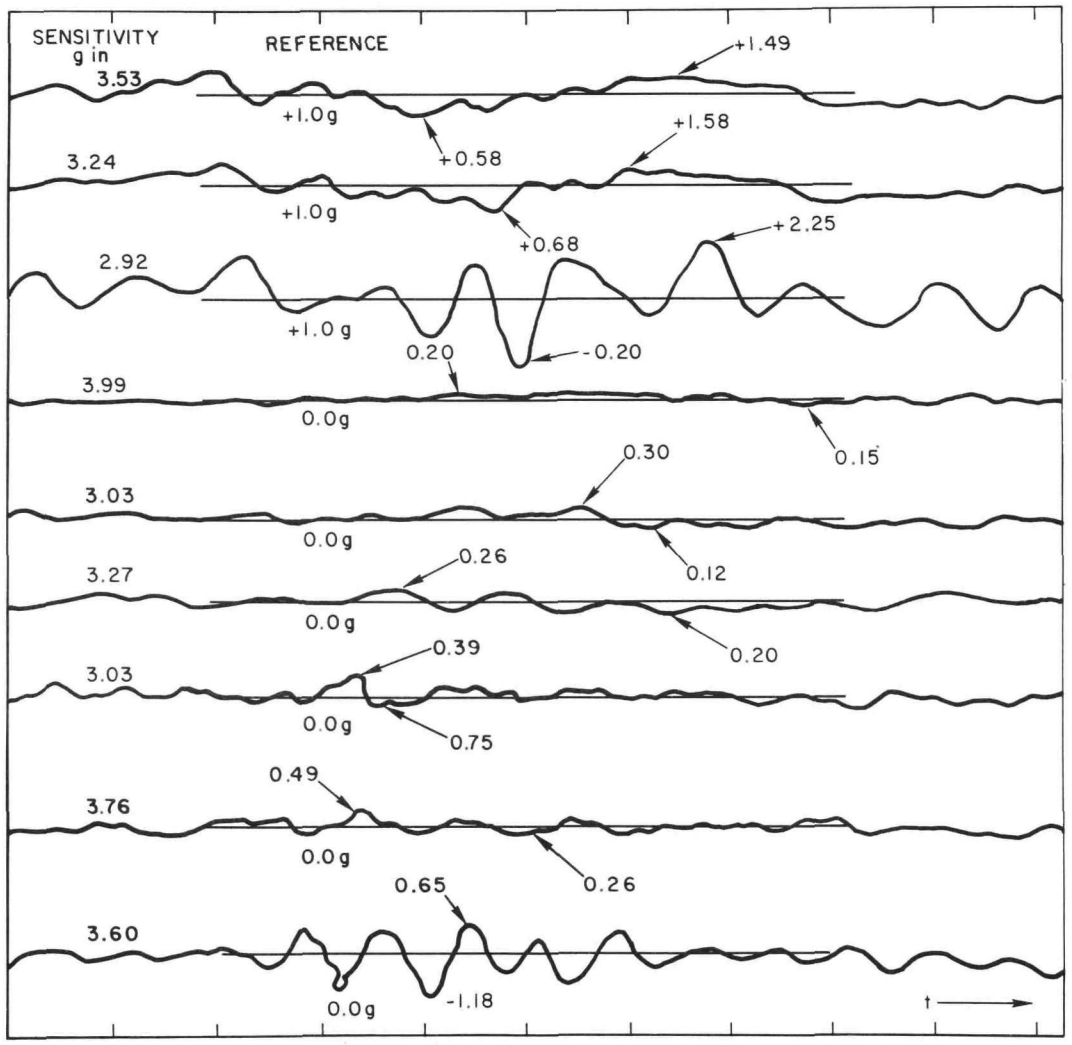

VERTICAL

Sled Aft

Sled Forward

Mass Mockup

LATERAL

Sled Aft

Sled Forward

Mass Mockup

LONGITUDINAL

Sled Aft

Sled Forward

Mass Mockup

Time 0.10 sec

4-1-64

7561-01277

Figure 30. Highway Transportation Test Results (1 of 2)

Oscillogram No. 727
Location: Devonshire St. at Zelzah Ave.
Road Condition: Transition from concrete to asphalt

Maximum Acceleration:					
Vertical	Positive	2.34 g	Negative	0.30 g
Lateral	Right	0.46 g	Left	0.20 g
Longitudinal	Fore	1.76 g	Aft	1.33 g

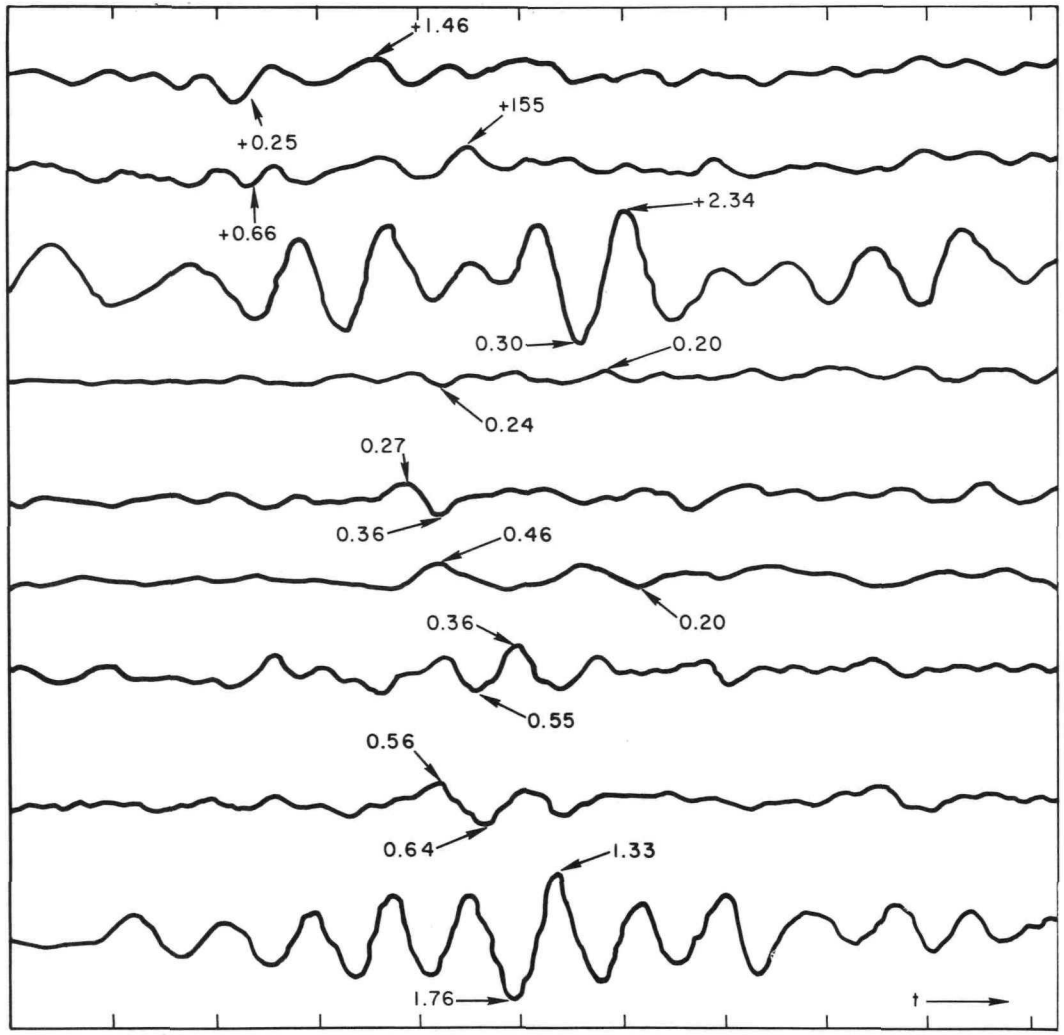

4-1-64

7561-01277

Figure 31. Highway Transportation Test Results (2 of 2)

IV. SNAP 10A–PSM–1 SLED TEST PROGRAM

A. INTRODUCTION

To investigate the feasibility of qualifying the SNAP 10A system structure under specified acceleration loading requirements, a rocket sled test program was initiated at the Edwards Air Force Experimental Track Facility, using the Atomics International rocket sled with a S10A mass mockup test vehicle aboard (Figures 32 and 33). A run made on February 6, 1962, indicated that for a 100% qualification run (1) the required acceleration was programmed within 5% of specified values, (2) the programmed acceleration level was sustained at subsonic levels for approximately 1.75 sec, (3) acceleration variation over the 1.75 sec test range did not exceed ±5% of the maximum acceleration, and (4) vibration levels measured at the vehicle's center of gravity did not exceed 3.7 g vertical, 3.8 g longitudinal, and 14.0 g lateral. All the results of this run (Figures 34 through 36), with the exception of the 14.0 g load at the center of gravity indicated that the testing method could be a satisfactory way of applying the specified acceleration loads.

B. TEST PROCEDURE

During the first run, the base portion of the test vehicle was firmly bolted to the shock-mounted support cradle, but the forward end was free to move with respect to the cradle in both the longitudinal and lateral directions. A simple restraint on the cradle prevented vertical motion between the cradle and the dummy test vehicle. Because the cradle and test vehicle were canted 7.5° laterally in the sled, the suddenly applied acceleration forces could impart considerable lateral deflection to the test unit and/or cradle. Post-run examination after Run No. 1 indicated that such was the case and that such contact was the probable cause of the few but undesirable cycles of lateral vibration noted at the start of the first run (Figure 36). To eliminate the possibility of abrupt contact of the vehicle's forward structure with the support cradle during the second run, more clearance between the test vehicle and the support cradle was provided. This was accomplished by (1) removing material from the forward support structure where interference was likely, and (2) reducing slightly the cant of the vehicle in the support cradle so that still more clearance would result

2-7-62

7580-18144

Figure 32. Rocket Sled Utilized for PSM-1 Acceleration Studies

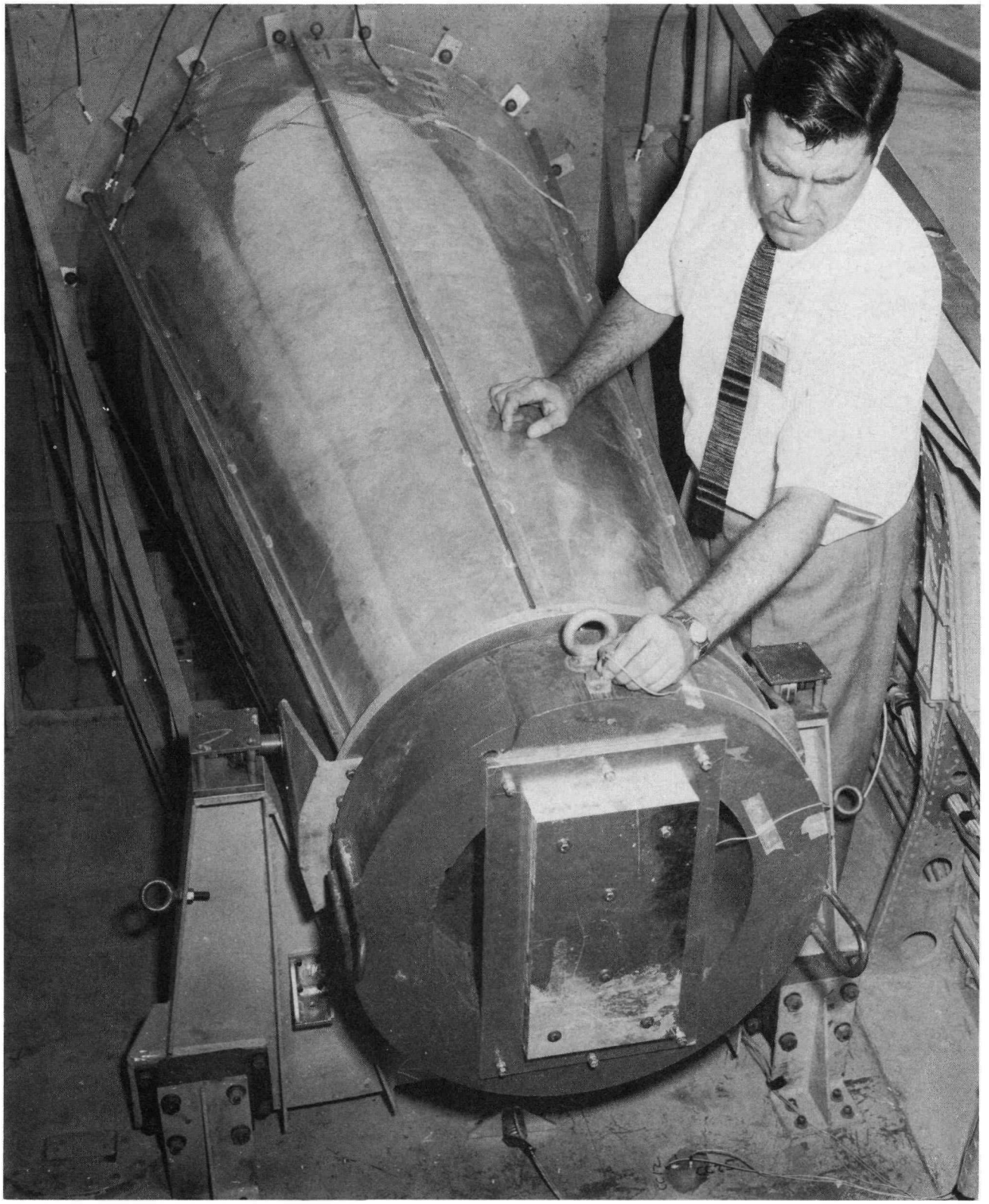

2-8-62

7580-18114

Figure 33. Dummy Structure Used in Sled Test Program

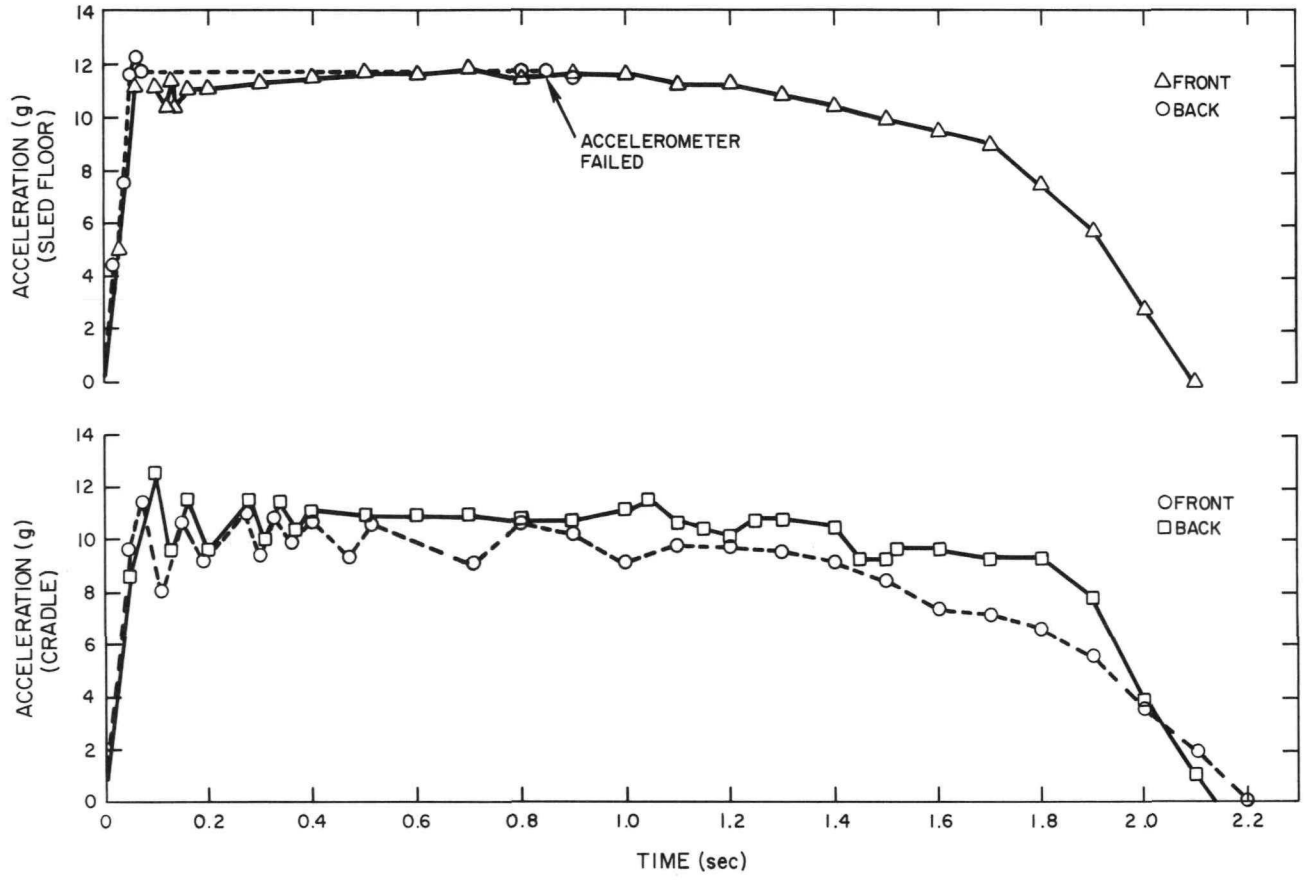

4-15-64

7561-01279

Figure 34. Sled Longitudinal Acceleration (Run No. 1)

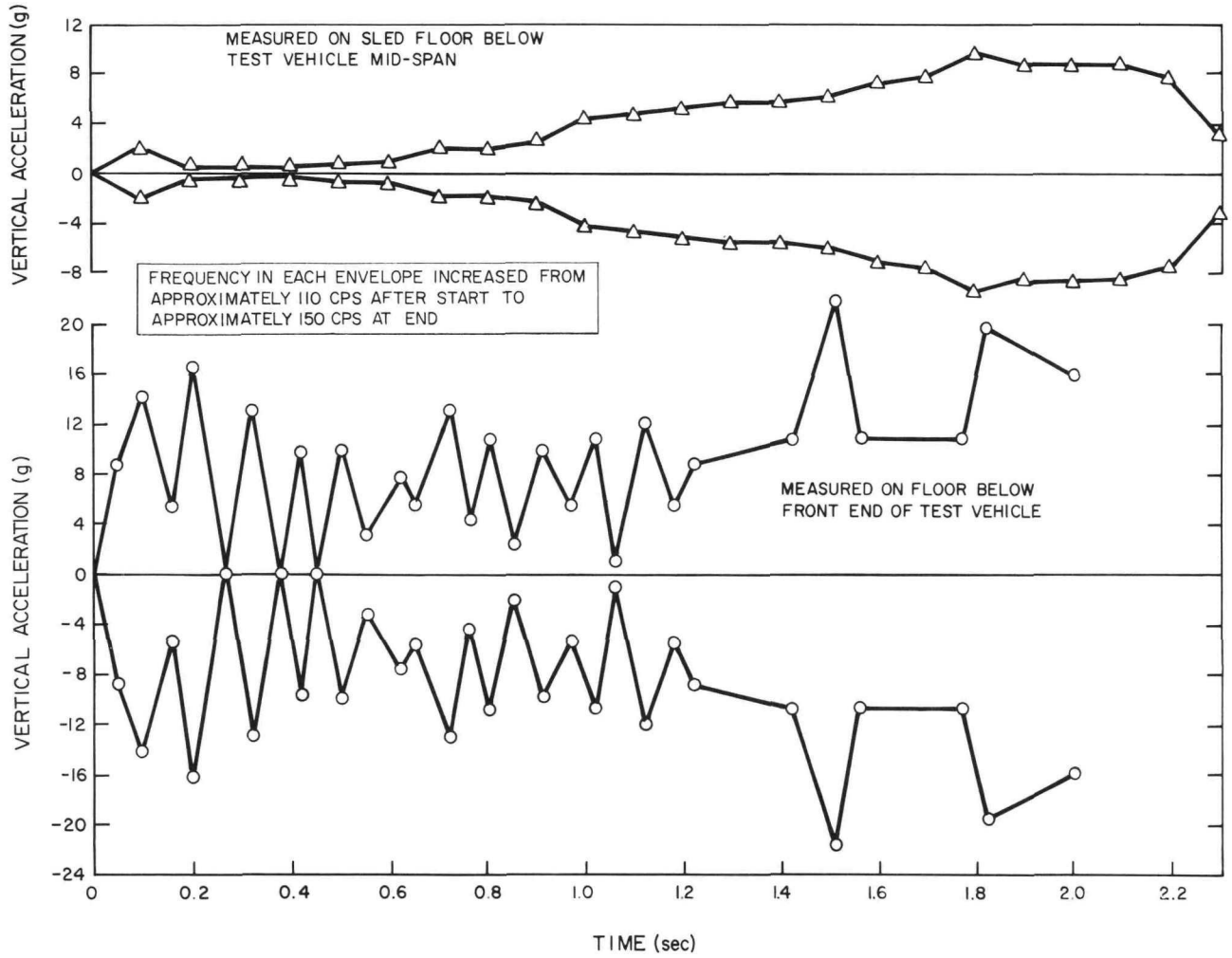

4-15-64 7561-01280

Figure 35. Acceleration Levels (Vibration) — Sled Floor (Run No. 1)

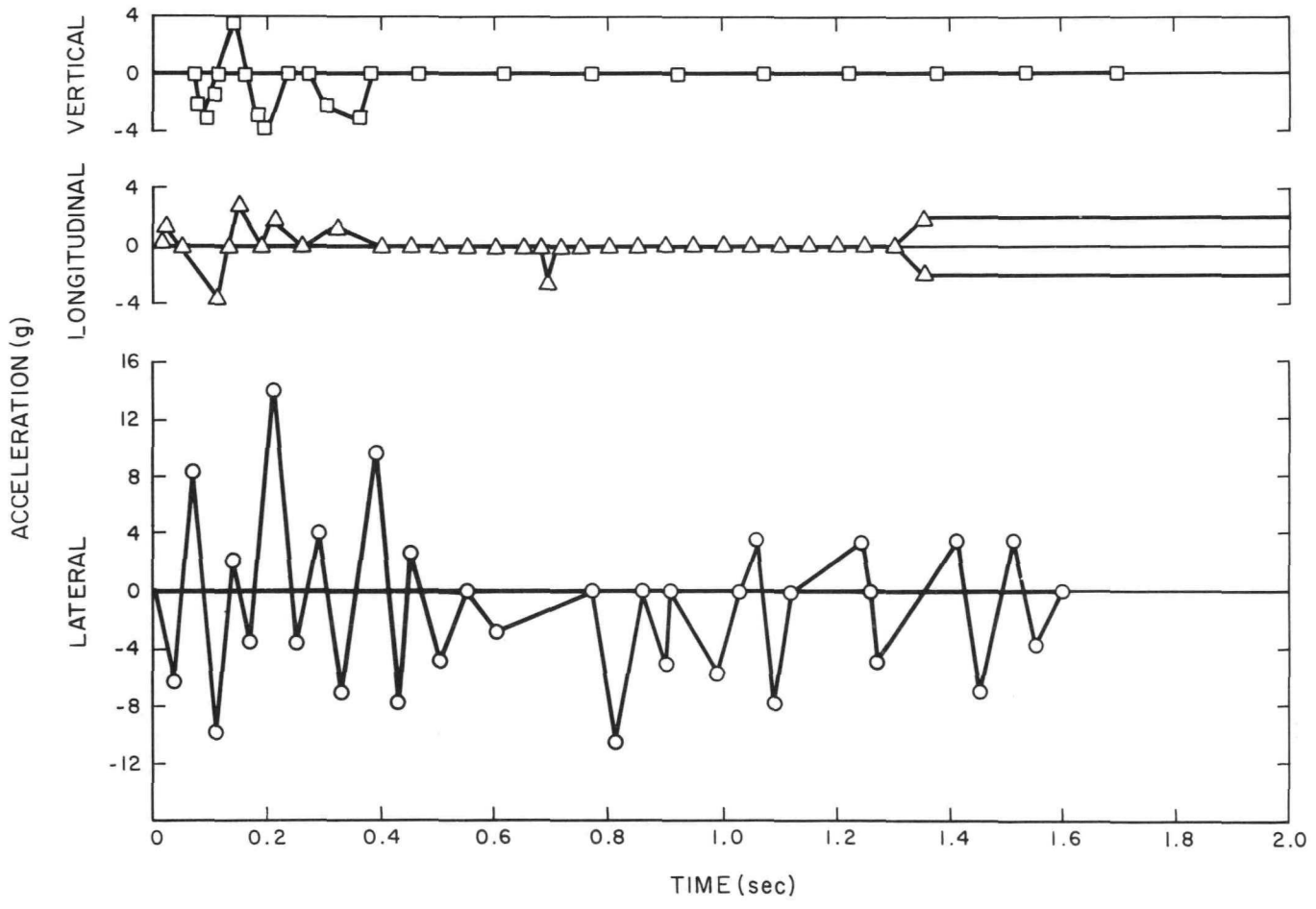

4-15-64

7561-01281

Figure 36. Acceleration Levels Measured at the Mass Mockup C. G. (Run No. 1)

at the forward end of the vehicle. Since the shock mount system cushioning the cradle from the sled floor seemed adequate, no changes were incorporated for the second run.

During the first sled run, the booster sled used for sled propulsion was firmly bolted to the aft end of the Atomics International sled, (Figure 32). Because the booster sled did not have shock-mounted rail slippers, it was felt that rail-induced vibration from this sled was needlessly transmitted to the test sled. Consequently, for the second run the booster was not attached and was in fact separated at the sled interfaces by a layer of heavy rubber.

To better survey the sled, cradle, and test vehicle responses during the second run, additional instrumentation was installed. Figure 37 indicates the location of all vibration sensors installed. For visual coverage, two high-speed movie cameras were installed in the sled housing forward of the test vehicle.

C. RESULTS

The acceleration of the rocket sled and the test vehicle is shown on Figure 38 and compared with the results of the first run. The oscillation at the start of the run is due to the unfortunate choice of having the two sleds unattached and, additionally, having them separated by the rubber bumper. Such oscillation was not evident in the first run when the two sleds were bolted together. Excellent sled-borne colored movie coverage showing the response of the dummy test unit to this oscillation was obtained.

A rocket bottle programing error by Edwards personnel caused the acceleration step at 0.5 sec. To generate a smooth acceleration rise time, a rocket bottle was to fire 0.05 sec after ignition of the first stage; but, because the figure was misread as 0.5 by a propulsion technician, the rocket bottles were incorrectly programmed. This error caused a 25 to 30% reduction in the intended 9.5 g steady-state acceleration over the first 0.55 sec of the run (See Figure 38).

Figure 38 also shows the longitudinal acceleration values recorded on the front of the dummy unit as well as on the base of the structure. The vibration levels superimposed on the acceleration curve represent the effect of the dummy rocking in the sled at the resonant frequency of the shock-mounted, cradle-dummy system.

VIBRATION		ACCELERATION	
NO.	FIG NO.	NO.	FIG NO.
1	4	A	*
2	4	B	*
3	4	C	*
4	*	D	*
5	*	E	3
6	*	F	*
7	*	G	2
8	5	H	3
9	5	J	*
10	5	K	2
		L	2

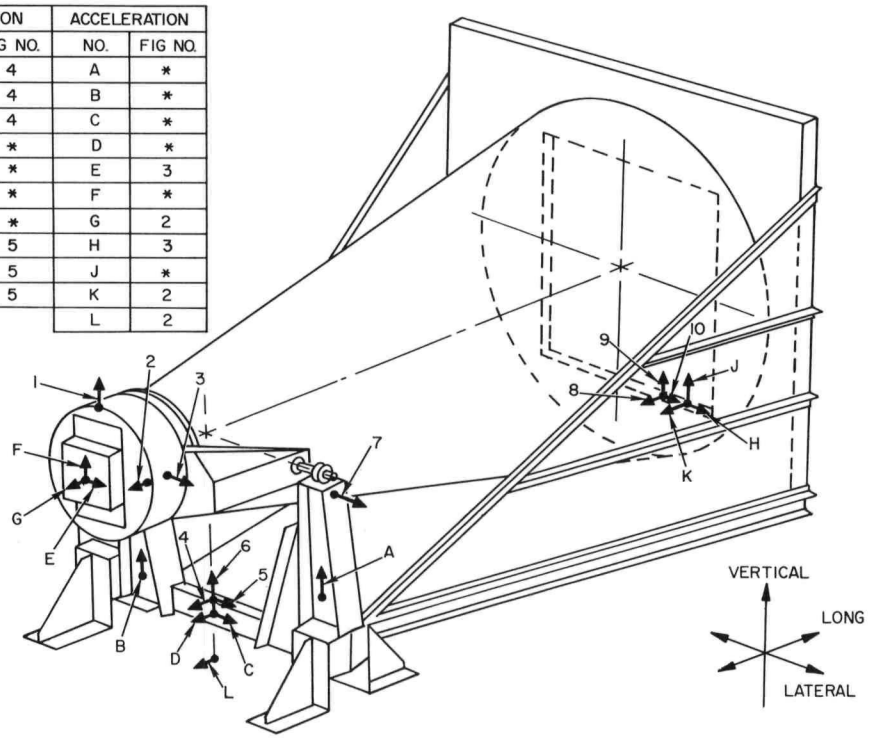

* NOT INCLUDED WITH THIS REPORT

4-15-64 7561-01282

Figure 37. Instrumentation Location for Sled Test Run

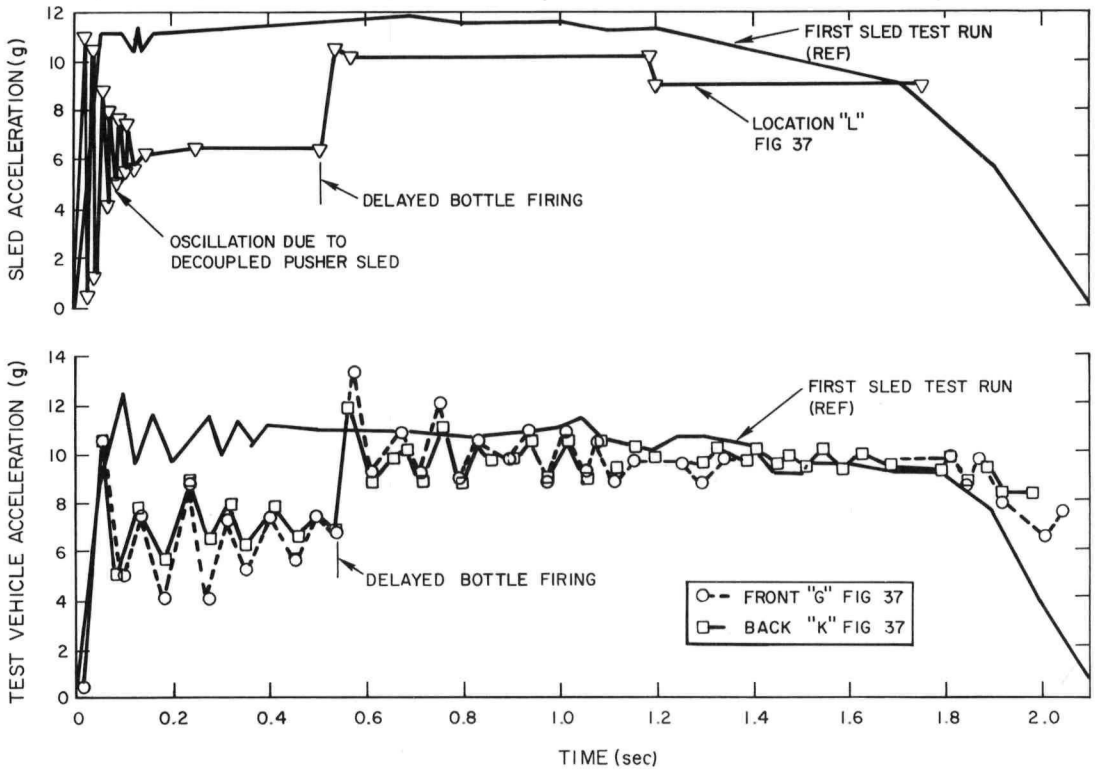

4-15-64 7561-01283

Figure 38. Sled and Test Vehicle Longitudinal Acceleration

The lateral acceleration of the dummy forward and base sections is noted in Figure 39. Because of the test unit cant, acceleration at the two ends is opposite. Steady-state acceleration levels in the vertical direction were found to average 0.5 g down at the front end of the test unit and 1 g up at the rear of the dummy structure.

In spite of the faulty rocket bottle programming, satisfactory results in terms of vibration levels were obtained at the vehicle center of gravity; in particular, the vibration levels in the lateral direction were reduced from those observed during the first sled run. Figure 40 shows plots of vibration levels in the forward section of the vehicle in the vertical, longitudinal and lateral directions. The only objectionable peaks occur in the longitudinal direction, where one -5.7 g and one +5.1 g peak were evident and, in the vertical direction, where one -5.5 g peak was noted. The cause of these three peaks was probably due to the high longitudinal vibration inputs imparted by the test sled and booster sled interface problem during the first 0.1 sec of test and could easily be eliminated by returning to the bolted steel-to-steel contact between the two sleds. The vibration levels observed at the sensor locations on the base of the test vehicle are noted in Figure 41.

On the basis of results from the two test runs, it was apparent that the vehicle support cradle and associated shock mount system were adequate to isolate the test unit from the excessive vibration levels induced by the sled.

It was concluded that if (1) the noted vehicle shock isolation system was employed, (2) a test run with a 9.5 g (125% of specification values) constant acceleration was programmed, (3) the booster sled was bolted directly to the test sled, and (4) the rocket bottles experienced no unusual malfunction, the following test results would be forthcoming:

1) The acceleration rise time would be $0.05 \, ^{+0.05}_{-0}$ sec

2) The sustained acceleration would be $9.5 \text{ g} \, ^{+0.5}_{-0}$ g

3) The test vehicle center of gravity lateral acceleration would be $9.5 \text{ g} \, ^{+0.3}_{-0}$ g

4) The time at the specified acceleration would be $1.75 \, ^{+0.2}_{-0.1}$ sec

5) The sled deceleration would not exceed 2.5 g

6) The vibration levels experienced at the test vehicle center of gravity would not exceed 5 g in any of three orthogonal axes.

No further sled test runs were conducted. The PSM-1 unit during the course of sled testing had been damaged during vibration tests and had subsequently been repaired for use in special vibration tests. It was not felt that the reworked unit was representative of a sound structure and so acceleration results on such a unit (if failure resulted) would be meaningless. Additionally, the PSM-1R structure was further obsoleted by the fact that a newer version, PSM-1A, was about to be delivered for test evaluation.

Any consideration for testing the PSM-1A vehicle on a rocket sled was discarded when it was learned that the Edwards Air Force Base Experimental Track Branch facility was scheduled for permanent closing at about the same time as the anticipated delivery for the PSM-1A unit. Because of the many problems which would be involved in transferring test activities to another facility, an alternate means of simulating acceleration loadings was specified. Static testing would be used in lieu of sled testing on all future SNAP 10A systems.

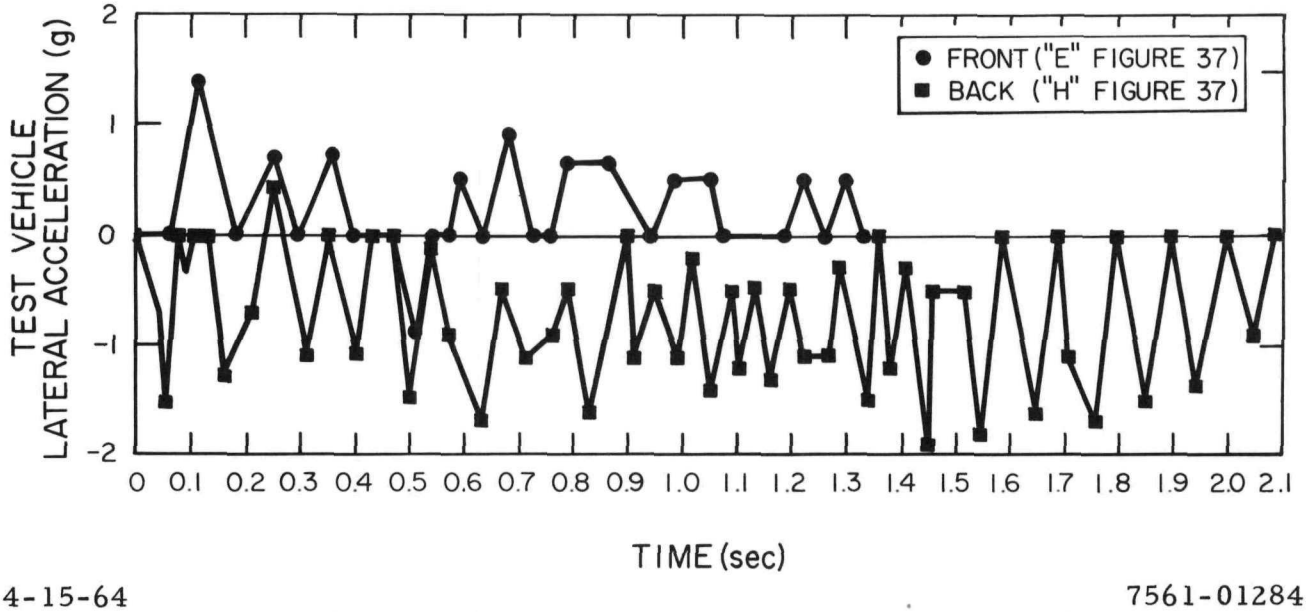

4-15-64 7561-01284

Figure 39. Test Vehicle Lateral Acceleration, Test No. 2

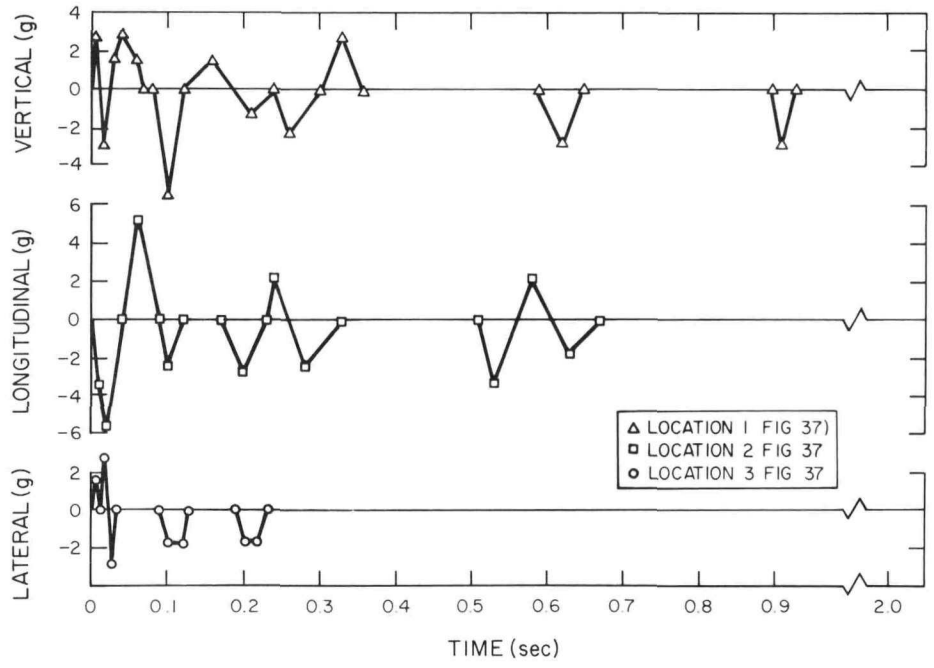

4-15-64 7561-01285

Figure 40. Test Vehicle Vibration Levels - Front, Run No. 2

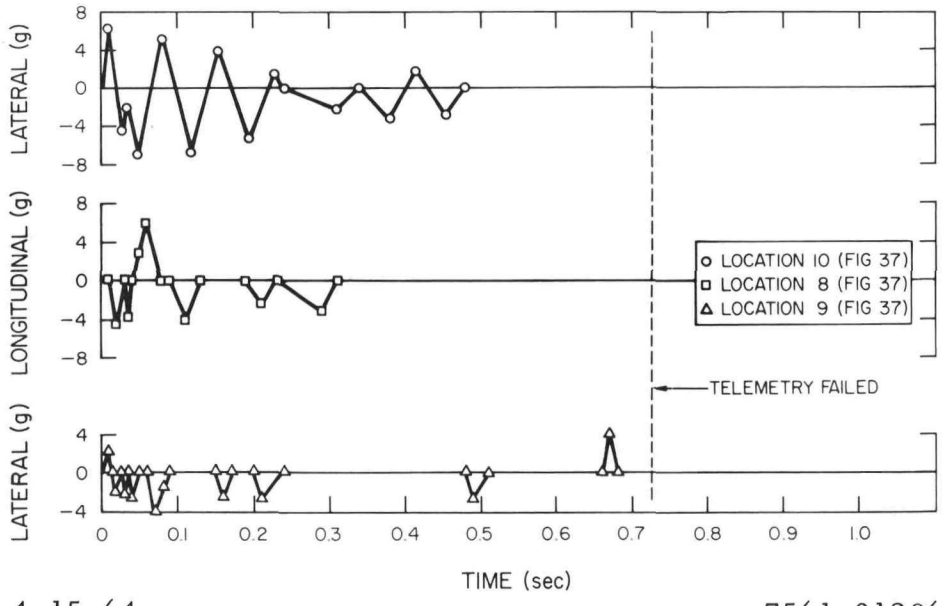

4-15-64 7561-01286

Figure 41. Test Vehicle Vibration Levels - Back, Run No. 2

BLANK

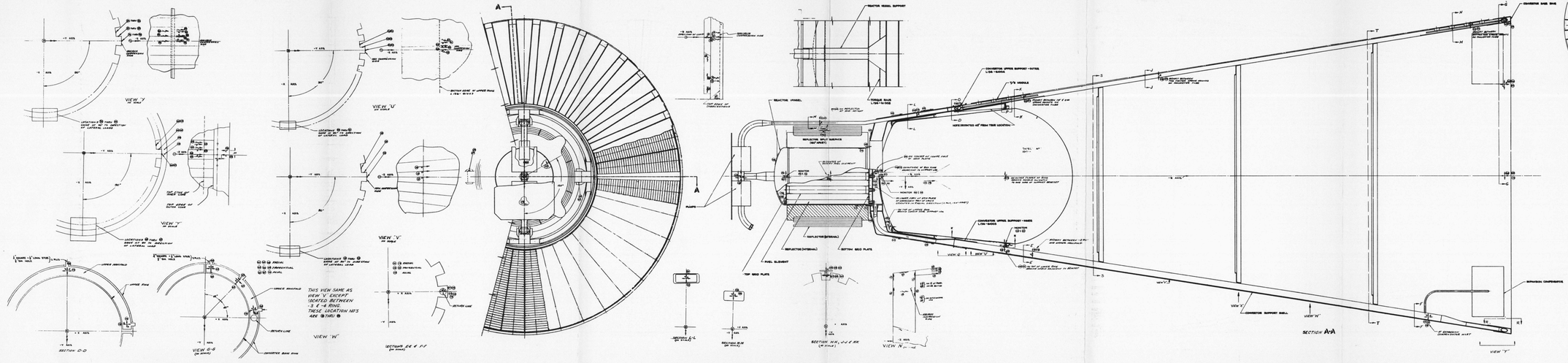

4-1-64 7561-01287

Figure 42. Additional Details for Location and Sensors

NAA-SR-8399

87